

# Status of the L2 and Lunar Charged Particle Environment Models

Joseph I. Minow\*

NASA Marshall Space Flight Center, Huntsville, AL 35812 USA

Anne M. Diekmann† and William C. Blackwell, Jr.‡

Jacobs Engineering, Marshall Space Flight Center Group, Huntsville, AL 35812 USA

The L2 Charged Particle Environment (L2-CPE) model is an engineering tool which provides free field charged particle environments for distant magnetotail, magnetosheath, and solar wind environments. L2-CPE is intended for use in assessing contributions from low energy radiation environments (~0.1 keV to few MeV) to radiation dose in thin materials used in construction of spacecraft to be placed in orbit about the Sun-Earth L2 point. This paper describes the status of the current version of the L2-CPE model including structure of the model used to organize plasma environments into solar wind, magnetosheath, and magnetotail environments, the algorithms used to estimate radiation fluence in sparsely sampled environments, the updated graphical user interface, and output options for flux and fluence environments. In addition, we describe the status and plans for updating the model to include environments relevant to lunar programs.

## I. Introduction

Particles with energies from a few eV through 1 MeV interacting with spacecraft surfaces and thin materials used in spacecraft construction produce a number of effects which must be considered by the spacecraft designer including spacecraft charging and degradation of material surfaces. Standard radiation environment models used to characterize and define radiation environments for the Sun-Earth/Moon L2 environment 236 Earth radii (Re) from the Earth in the anti-solar direction typically emphasize the high energy, penetrating component of the space environment. Solar proton event models [Feynman *et al.*, 1990, 1993, 2002; Xapsos *et al.*, 1999, 2000; Jun *et al.*, 2006] and the Cosmic Ray Effects on Microelectronics code [Tylka *et al.*, 1997] are widely used by radiation effects engineers for evaluating dose on spacecraft in interplanetary space but are primarily directed towards understanding the impact of solar particle events (SPE) and galactic cosmic rays (GCR) on electronic systems when planning missions for L2. These models are not appropriate for the low energy plasma populations in the solar wind, magnetosheath, magnetotail, and the low energy component of SPE's. The L2-Charged Particle Environment (L2-CPE) model (Figure 1) was developed to meet this need.

The origin of the L2-CPE model is the preliminary L2 Radiation (LRAD) engineering

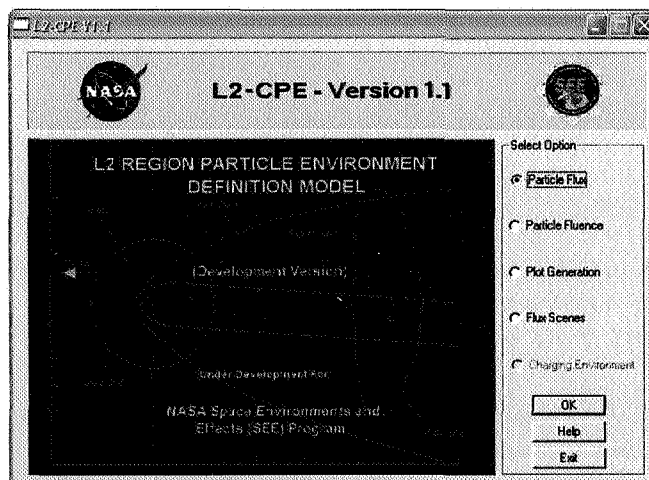


**Figure 1. L2 CPE Model.** The entry screen of the current version of the L2-CPE model provides options for users to evaluate flux and fluence, plot results, or generate scenes of distant magnetotail plasma regimes.

\* AST, Flight Vehicle Space Environments, Spacecraft and Vehicle Systems Department, NASA/MSFC/EV13, Huntsville, AL, Senior Member.

†Analyst, Environments Team, Jacobs Engineering, MSFC Group, Huntsville, AL.

‡Engineering Specialist, Environments Team, Jacobs Engineering, MSFC Group, Huntsville, AL.

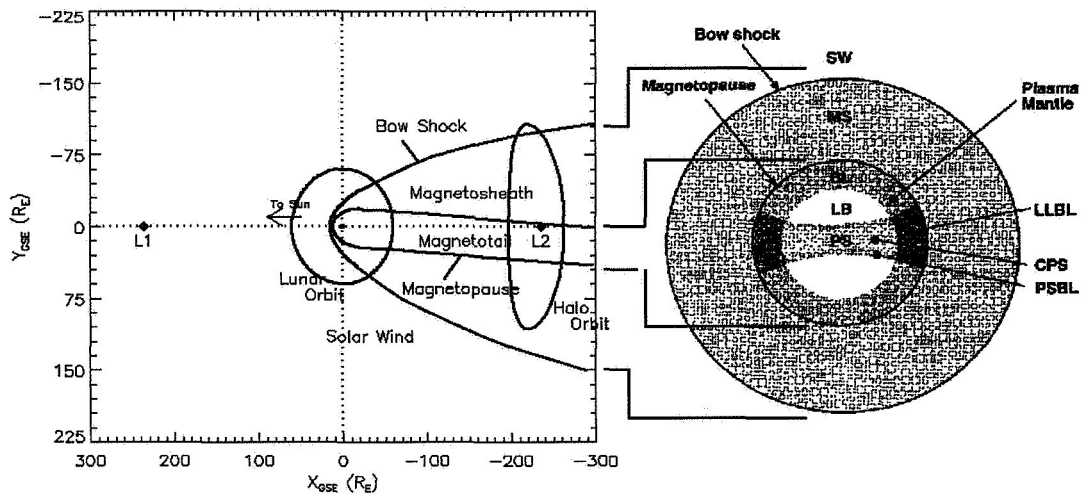


**Figure 2. Magnetotail Plasma Environments.** Plasma regime boundaries of the Earth-Moon system projected onto the ecliptic geocentric solar ecliptic (GSE) X-Y plane. The first and second Lagrange points, L1 and L2, are located  $\sim 236 R_e$  from the Earth along the Earth-Sun line. A sample halo orbit about L2 is shown to demonstrate the magnitude of potential orbital amplitudes about L2 relative to the dimensions of the magnetotail and magnetosheath at L2 distances. Spacecraft in orbit about L2 can sample a range of plasma regimes including the solar wind (SW), magnetosheath (MS), boundary layer (BL), lobe (LB), plasma sheet (PS), low latitude boundary layer (LLBL), central plasma sheet (CPS), and plasma sheet boundary layer (PSBL) (adapted from Minow et al., 2000).

model [Blackwell et al., 2000; Minow et al., 2000] developed to provide estimates of thermal plasma flux and fluence spectra for spacecraft in halo orbits about L2, providing the information necessary for analysis of particle populations responsible for surface degradation and charging effects (through energies of a few tens keV) not available in the current SPE and GCR models. NASA's Space Environments and Effects (SEE) Program sponsored a significant development of the LRAD model currently known as the L2 Charged Particle Environment Model (L2-CPE) as well as an extension of the model to include environments relevant for lunar missions. This paper provides a status of the L2-CPE model as well as current efforts to complete the Luna Charged Particle Environment Model (Luna-CPE).

## II. L2 Charged Particle Environment Model

Spacecraft in large amplitude halo orbits about L2 sample a wide range of plasma regimes during a single orbit. Although each orbit is on the order of six months, on shorter time scales the spacecraft may sample any of the distant magnetotail plasma regimes due to the great variability in the orientation of the magnetotail. Figure 2 demonstrates the nominal orientation of the magnetotail due to the combined effects of the average solar wind flow and the orbital velocity of the Earth. Extreme cases of large or small solar wind velocities result in large shifts of the magnetotail. Since time scales of solar wind variations are on the order of tens of minutes to hours, interactions with the distant magnetotail are possible during the entire halo orbit.

The solar wind driven variability in the dimensions and orientation of the distant magnetotail is an important consideration in determining which plasma regimes a satellite will most often encounter near L2. Plasma data acquired by a satellite in the vicinity of the deep tail Sun-Earth line cannot simply be assumed to be magnetotail plasma for this reason. Similarly, spacecraft halo orbits will bring the satellite into contact with a variety of plasma regimes due to the combined effects of the variable magnetotail orientation and dimensions as well as the time varying position of the satellite along the orbit. Solar wind encounters are most likely at the furthest excursions from the Sun-Earth line when the satellite is nearest the bow shock. Magnetotail encounters will be the most likely

for locations along the orbit closest to L2. In either case, the entire set of plasma regimes (solar wind, magnetosheath, and magnetotail plasmas) may be encountered depending on the solar wind conditions.

An assessment of L2 plasma conditions requires simultaneous consideration of bow orbital motion of the spacecraft, the plasma boundaries, and the individual variations within these plasma regimes. For example, rapid variability of the magnetotail and magnetosheath on minute time scales--much less than typical six month halo orbit period--requires the solar wind dependent variability to be treated for all times throughout a halo orbit. Computation of particle flux within individual plasma regions and fluence for complete halo orbits is accomplished in the LRAD model providing a framework for incorporating statistical variations in plasma parameters and fluctuations in magnetotail structure and position due to time dependent variations in the solar wind.

The SEE Program sponsored an update of the LRAD code which resulted in the current version of the L2-CPE model. A number of number of modifications of the LRAD model are incorporated into the L2-CPE code. First, the distant magnetotail charged particle environment model was changed from the original text based, command line input version to a new format for use with a graphical user interface (GUI). The Winteractor Fortran 90/95 toolset was used to develop the GUI driver for running the modified code. Figure 1 is the starting screen from the model using the Winteractor GUI driver. Although a number of options for developing the driver were considered, the Winteractor toolset was chosen at the time the driver was developed because it provided the development team the convenience of bundling the core model with the modified flux reconstruction software and the graphical display features into a single Fortran executable. The resulting model is therefore easy to distribute as a single executable along with the required plasma regime databases the software utilizes to characterize the flux and fluence environments.

L2-CPE and its LRAD predecessor are empirical models based on electron and ion (proton, helium) moments derived from differential flux measurements in the distant magnetotail and solar wind. Data sources are given in Table 1. The original database used in the LRAD model was based on a six month time series of Geotail Comprehensive Plasma Instrument (CPI) Hot Plasma Analyzer (HPA) cold plasma moments from the first half of 1993 and then only records within 25 Re of the Earth-Sun line. The first database update incorporated into L2-CPE was to obtain the full set of late 1992 through the end of 1994 CPI/HPA records to fill out the database providing better coverage for not only additional magnetotail encounters but magnetosheath sampling as well. The Geotail data set does not provide extensive solar wind sampling at distances beyond -50 Re so ion moments from the Interplanetary Monitoring Probe (IMP) 8 Faraday cup were used for solar wind environments instead. In addition to providing the solar wind plasma environments for fluence estimates, the IMP-8 data set is used to drive the solar wind dependent orientation and dimensions of the magnetotail and magnetosheath.

LRAD only provided for flux reconstruction using cold plasma moments and Maxwellian distribution functions. This was adequate to represent the peak of the ion flux distributions and the core of the electron distributions but did not adequately represent the non-thermal particle distributions through MeV energies. A significant modification included in the L2-CPE model was the addition of electron and ion flux environments represented by kappa distribution functions [Minow *et al.*, 2004, 2005]. Cold plasma moments are used for the number density, temperature, and convection velocity inputs to the kappa distribution functions and the kappa parameters adjusted until the non-thermal flux matches the measurements at 10's to 100's keV. The non-thermal tails of the distribution functions are constrained by energetic ion and electron flux provided by the Energetic Particle and Ion Composition (EPIC) Ion Composition Subsystem (ICS) instrument onboard the Geotail spacecraft.

**Table 1. L2-CPE Data**

Database	Number of Records	
	LRAD	L2-CPE
<b>Solar Wind</b>		
--IMP 8 solar max	105,120	105,120
--IMP8 solar min	105,120	105,120
--Ulysses solar max	----	32,342
--Ulysses solar min	----	25,106
<b>Magnetosheath</b>		
--Geotail	2,649	212,426
<b>Plasma mantle</b>		
--Geotail	10,148	99,420
<b>Plasma sheet</b>		
--Geotail	8,605	71,752

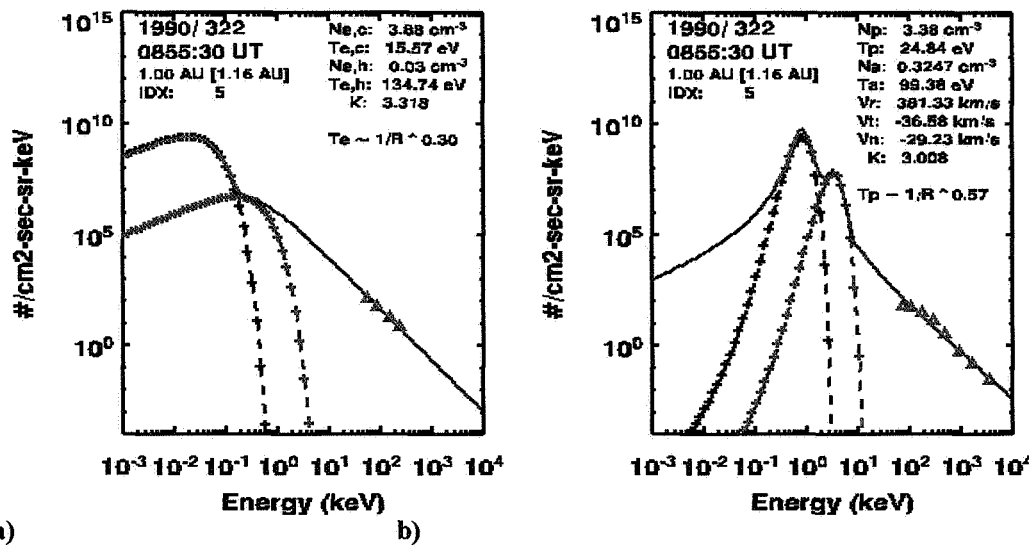


**Figure 3. Flux Reconstruction.** Example of reconstructed (a) electron and (b) ion differential flux using Ulysses data scaled to 1 AU. The green curve is the final fit obtained by modifying the kappa parameter until the derived flux matches the observed energetic particle measurements.

The data set provided by the instrument Principal Investigator (PI) at the Johns Hopkins University/Applied Physics Laboratory was a complete set of the azimuthally resolved differential flux measurements for the period corresponding to the CPI/HPA records. These records were averaged into flux arriving from four sunward, antisunward, dawnward, and duskward quadrants for use in the model database. Although a similar energetic particle data set from the Charged Particle Measurement Experiment (CPME) instrument on the IMP-8 satellite is available to constrain the solar wind distribution functions, to date we have only used average values of the kappa function reported in the scientific literature to provide the solar wind database [Minow *et al.*, 2005]. The final analysis and processing routines (Figure 3 is from the processing routine diagnostics package) provide a capability to effectively merge the EPIC/ICS energetic ion and IMP-8/CPME electron flux measurements with low energy Geotail Comprehensive Plasma Instrument (CPI) Hot Plasma Analyzer (HPA) plasma moments (number density, temperature, and velocity) and IMP-8 Faraday cup ion moments to yield a single, comprehensive differential ion and electron flux over an energy range of from 10 eV through 1 MeV.

A significant issue encountered in building the model is the sparse sampling of the distant magnetotail during the first two years of the Geotail mission shown in Figure 4. In addition, spacecraft orbiting L2 sampling the distant magnetotail plasma regimes with a different geometry than that provided by the elliptical Geotail orbits. In order to optimize the use of the sparse Geotail plasma records and provide a method for sampling distant magnetotail plasma regimes along orbits not sampled by Geotail, we have adopted a random sampling technique to build up fluence during integrations along orbits in the model. The technique approximates the flux along the spacecraft orbit by Monte Carlo sampling the relevant plasma regime database along the orbit. Over long periods of time (multiples of halo orbit periods) the technique provides an adequate representation of fluence environment along the

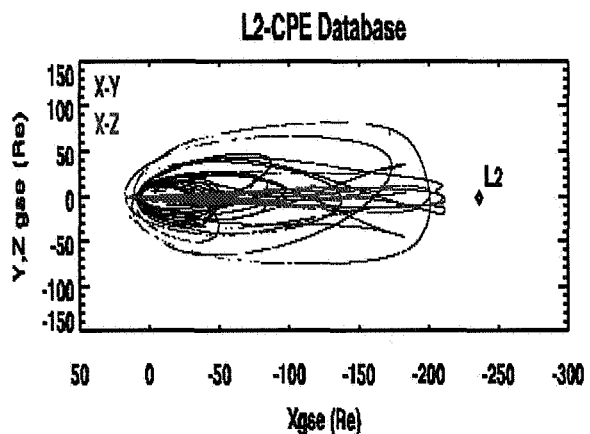


**Figure 4. L2 CPE Distant Magnetotail Database.** Geotail orbits from launch in late 1992 through the end of 1994 are shown here to demonstrate the sparse coverage of magnetotail environments beyond -100 Re from the Earth.

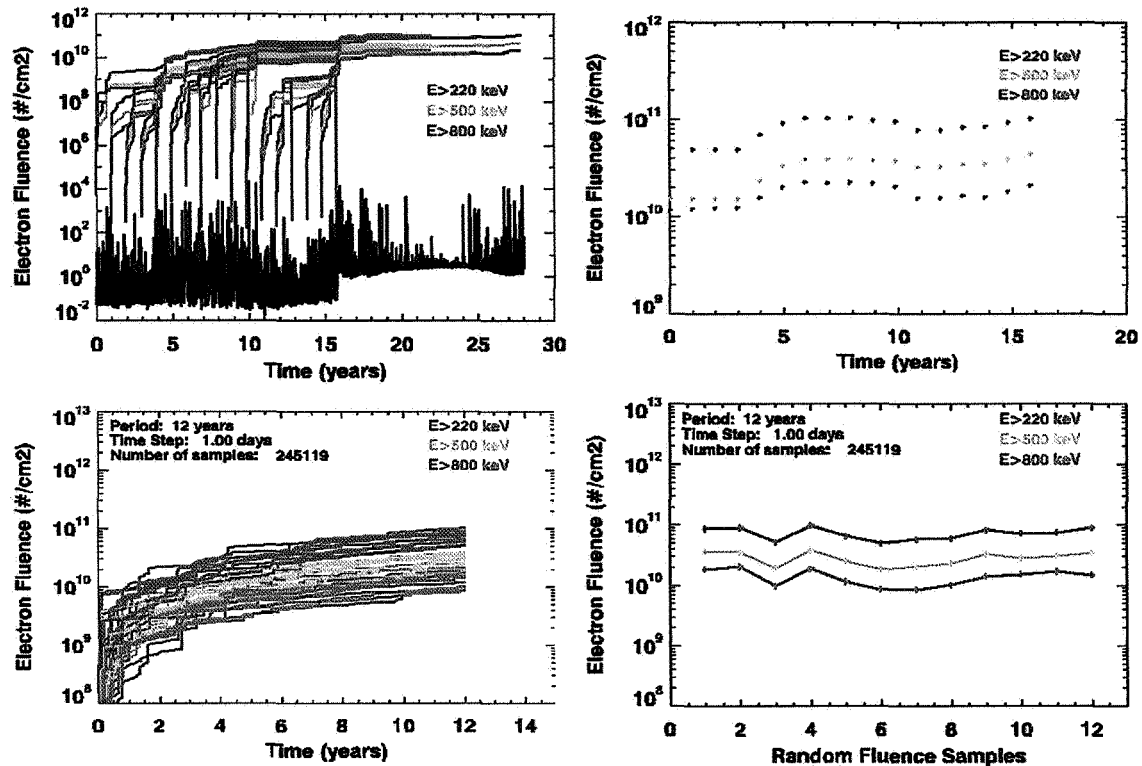
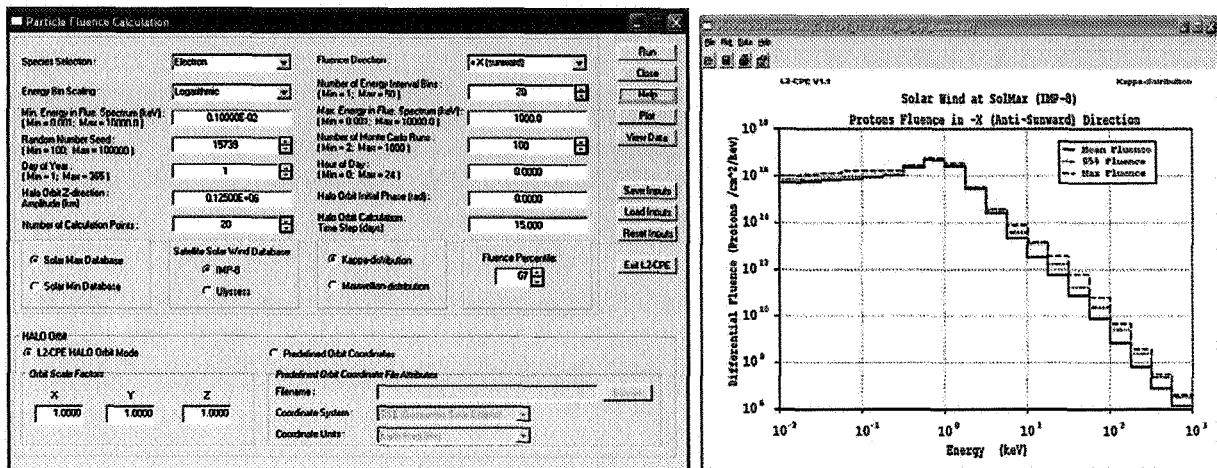


**Figure 5. CPE Data Sampling Technique.** Exact (top panels) and random sampling (bottom panels) fluence estimates using IMP-8 energetic electrons as an example. Colored lines in the top left panel show the integrated 12 year fluence started at one year intervals for the indicated integral electron channel. Fluence results in the top right panel are 12 year integration results for a variety of start times. Accumulated fluence estimates in the bottom left panel are obtained by random sampling of the IMP-8 data set and the corresponding 12 year fluence results are given in the bottom right panel.

spacecraft orbit.

Figure 5 provides an example of the random sampling technique using the IMP-8 Charged Particle Measurement Experiment (CPME) for clarity. CPME integral >220 keV electron flux is shown in the top left panel (black line) for a 28 year period from 1972 through 2000. Fluence estimates obtained by integrating time series of the CPME >220 keV (red), >500 keV (orange), and >800 keV (green) channels over 12 year periods are shown where the starting time for each of the individual fluence integrations are shifted by one year intervals. The top right panel shows only the final fluence values for a number of 12 year integration periods. In comparison, the bottom left panel shows 12 year fluence estimates obtained by random sampling the IMP-8 electron flux time series and integrating to obtain accumulated fluence. Final fluence values for the numerical experiments are given in the lower right panel. Comparing the range of exact 12 year solar wind fluence accumulations in the top right panel with the random sampled values in the lower right panel demonstrate the method provides good estimates of fluence over long periods of time. For example, the exact integral solar wind fluences for the >800 keV electron channel range from  $1 \times 10^{10} \text{ e}^-/\text{cm}^2$  to  $2 \times 10^{11} \text{ e}^-/\text{cm}^2$  and the random sampled version yield the same range of values.

The fluence analysis control screen is shown in Figure 5 along with an example fluence estimate output for a 12 year period. In the case of the L2-CPE model, the Monte Carlo sampling of the plasma regime data is modified by the changing orientation and dimensions of the magnetopause and bow shock. As the model steps along the spacecraft orbit about L2, a spacecraft regime (solar wind, magnetosheath, boundary layer, plasma sheet) is assigned to each step based on a modified version of the *Petrinec and Russell* [1993, 1996] magnetopause model and *Bennett et al.* [1997] bow shock model. The individual plasma databases are then randomly sampled using the technique just described in the IMP-8 example.



(a) (b)  
**Figure 6. L2 CPE Fluence Analysis.** (a) L2-CPE fluence screen controls user selected options for conducting fluence estimates along spacecraft orbits. (b) Example fluence results for a halo orbit about L2.

At the time of writing, the current version (L2-CPE Version 1.1) is still considered preliminary because the documentation and web-based help files are still being finalized but the model itself is currently available for use and is distributed by NASA's Environments Branch at Marshall Space Flight Center (<http://see.msfc.nasa.gov/>). Current plans are to freeze L2-CPE Version 1.1 and incorporate any further changes, updates, or corrections in the model in future versions of the software.

### III. Lunar Charged Particle Environment

The Lunar Charged Particle Environment (Luna-CPE) is an extension of the L2-CPE model which will include environments relevant to lunar missions. The magnetopause and bow shock models used in the original L2-CPE model are generally applicable over a range of distances from the subsolar point ~10 to 14 Re upstream of the Earth to L2 and beyond and no modifications were required to incorporate the lunar environments. Additional plasma records were added to fill out the database between the Earth and the Moon. L2-CPE includes 1992 through 1994 Geotail records for over the distance range of  $-50 \text{ Re} < X_{\text{GSE}} < -220 \text{ Re}$  which does include lunar orbit at ~60Re from the Earth. To supplement this database we have added the remaining Geotail records from the 1992 to 1994 period for distances less than 50 Re from the Earth and incorporated two additional years (1995 and 1996) of Geotail records after the spacecraft trajectory was modified to a 8 Re x 30 Re orbit. A lunar orbit generator providing options to orbit spacecraft about the Moon and sample plasma environments as the Moon moves around the Earth once a month has been incorporated into the code. The current version of the model requires a user to provide a spacecraft ephemeris for trans-lunar and trans-earth trajectories. Plasma densities and temperatures are greatly modified in the lunar wake to distances of some 20 to 30 lunar radii [Schubert and Lichtenstein, 1974; Olgilvie et al., 1996; Clack et al., 2004; Trávníček, 2005]. Finally, the lunar wake is currently being incorporated as a perturbation of the free field environment provided by the model. Lunar wakes are an important feature of the plasma environment in lunar space because spacecraft have been shown to charging to negative potentials of a few hundred volts within the lunar wake [Halekas et al., 2005].

Current plans are to release a beta version of the Luna-CPE model in late 2007.

### Acknowledgement

We gratefully acknowledge Dr. Richard McEntire and Stuart Nyland of the Johns Hopkins Applied Physics Laboratory for providing the Geotail EPIC records. CPI/HPA records were provided by Dr. L. Frank and Dr. W. Peterson of the University of Iowa. IMP8 plasma data was obtained from MIT courtesy Dr. A. Lazarus and Dr. K. Paularenus. Ulysses/SWOOPS moments and HISCALE energetic particle records were obtained courtesy of D.J. McComas and L. Lanzerotti, respectively, from the NASA National Space Science Data Center and the Space Physics Data Facility.

## References

- Bennett, L., M. G. Kivelson, K. K. Khurana, L. A. Frank, and W. R. Paterson, A model of the Earth's distant bow shock, *J. Geophys. Res.*, 102, 26927 – 26941, 1997.
- Blackwell, W.C., J.I. Minow, S.W. Evans, D.M. Hardage, and R.M Suggs, *Charged Particle Environment Definition for NGST: Model Development*, Proc. SPIE, 4013, 908-919, UV, Optical, and IR Space Telescopes and Instruments VI, J.B. Breckinridge and P. Jakobsen, eds., 2000.
- Clack, D., J.C. Kasper, A.J. Lazarus, J.T. Steinberg, and W.M. Farrell, Wind observations of extreme ion temperature anisotropies in the lunar wake, *Geophys. Res. Lett.*, 31, L06812, doi:10.1029/2003GL018298, 2004.
- Feynman, J., T. P. Armstrong, L. Dao-Gibner, and S. Silverman, New Interplanetary Proton Fluence Model, *J. Spacecraft*, Vol. 27 No. 24, pp 403-410, July-August 1990.
- Feynman, J., Spitale, G., and Wang, J. Interplanetary proton fluence model: JPL 1991, *J. of Geophy. Res.*, 98, pp. 13,281-13,294, 1993.
- Feynman, J., Ruzmaikin, A., Berdichevsky, V. The JPL proton model: an update, *Journal of Atmospheric and Solar-Terrestrial Physics*, 64(A8), pp. 1679-1686, 2002.
- Halekas, J.S., S.D. Bale, D.L. Mitchell, and R.P. Lin, Electrons and magnetic fields in the lunar plasma wake, *J. Geophys. Res.*, 110, A07222, doi:10.1029/2004JA010991, 2005.
- Jun, I., R.T. Swimm, A. Ruzmaikin, J. Feynman, A.J. Tylka, W.F. Dietrich, Statistics of solar energetic particle events: Fluences, durations, and time intervals, *Adv. Space Res.*, in press, 2006.
- Minow, J.I., W.C. Blackwell, Jr., and A. Diekmann, *Plasma Environment and Models for L2*, AIAA Paper 2004-1079, 42nd AIAA Aerospace Sciences Meeting and Exhibit, Reno, NV, 5-8 January 2004.
- Minow, J.I., W.C. Blackwell, L.F. Neergaard, S.W. Evans, D.M. Hardage, and J.K. Owens, *Charged Particle Environment Definition for NGST: L2 Plasma Environment Statistics*, Proc. SPIE, 4013, 942-953, UV, Optical, and IR Space Telescopes and Instruments VI, J.B. Breckinridge and P. Jakobsen, eds., 2000.
- Minow, J.I., L.N. Parker, and R.L. Altstatt, *Radiation and Internal Charging Environments for Thin Dielectrics in Interplanetary Space*, presented at the 9th Spacecraft Charging Technology Conference, Tsukuba, Japan, 4-8 April 2005.
- Ogilvie, K. W., J. T. Steinberg, R. J. Fitzenreiter, C. J. Owen, A. J. Lazarus, W. M. Farrell, and R. B. Torbert (1996), Observations of the lunar plasma wake from the Wind spacecraft on December 27, 1994, *Geophys. Res. Lett.*, 23, 1255–1258.
- Petrinec, S.M. and C.T. Russell, An empirical model of the size and shape of the near-Earth magnetopause, *Geophys. Res. Lett.*, 20, 2695 - 2698, 1993.
- Petrinec, S.M. and C.T. Russell, Factors controlling the shape and size of the post-terminator magnetopause, *Advances in Space Research*, 18, (8)213-(8)216, 1996
- Schubert, G., and B. R. Lichtenstein, Observations of Moon-plasma interactions by orbital and surface experiments, *Rev. Geophys.*, 12, 592–626, 1974.
- Trávníček, P., P. Hellinger, D. Schriver, and S.D. Bale, Structure of the lunar wake: two-dimensional global hybrid simulations, *Geophys. Res. Lett.*, 32, L06102, doi:10.1029/2004GL022243, 2005.
- Tylka, A.J., J.H. Adams, Jr., P. Boberg, B. Brownstein, W.F. Dietrich, E.O. Flueckiger, E.L. Petersen, M.A. Shea, D.F. Smart, and E.C. Smith, CREME96: A Revision of the Cosmic Ray Effects on Micro-Electronics Code, *IEEE Transactions on Nuclear Science*, 44, 2150-2160, 1997.
- Xapsos, M. A., G. P. Summers, J. L. Barth, E. G. Stassinopoulos, and E. A. Burke, Probability Model for Worst Case Solar Proton Event Fluences, *IEEE Trans. Nucl. Sci.*, 46, 1481-1485, 1999.
- Xapsos, M. A., G. P. Summers, J. L. Barth, E. G. Stassinopoulos, and E. A. Burke, Probability Model for Cumulative Solar Proton Event Fluences, *IEEE Trans. Nucl. Sci.*, 47, 486-490, 2000.

AIAA-2007-0910  
**Status of the L2 and Luna Charged  
Particle Environment Models**



Joseph I. Minow  
EV13/Natural Environments Branch  
NASA, Marshall Space Flight Center

Anne M. Diekmann and William C. Blackwell, Jr.  
Jacobs Engineering, MSFC Group  
NASA, Marshall Space Flight Center

*45<sup>th</sup> AIAA Aerospace Sciences Meeting  
Reno, Nevada 8-11 January 2007*

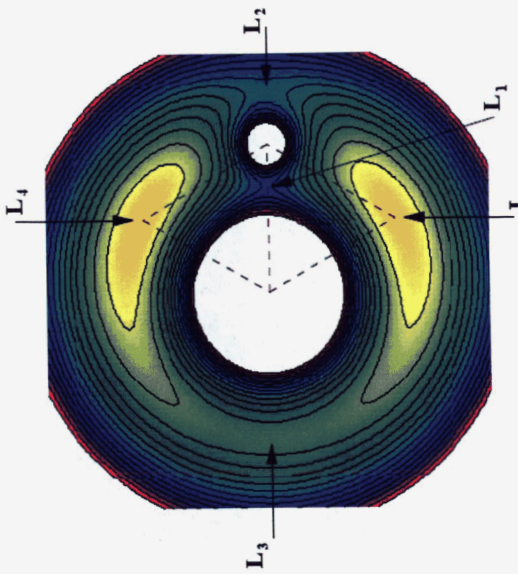






# Introduction

- Outline**
- Libration point geometry
  - L2 Charged Particle Environment Model
  - Lunar Update
  - Summary



(from Cornish and Goodman, 2006)

$V, dV/dt = 0$  at libration points

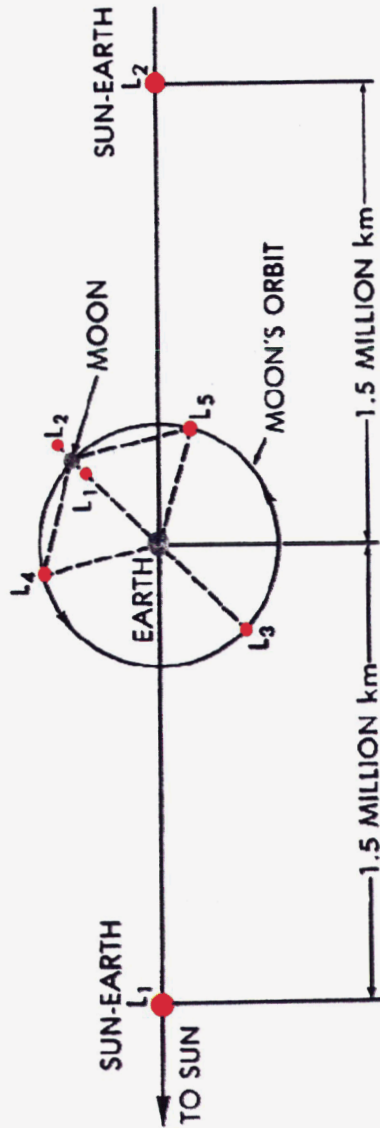
L1, L2, L3:

--Gravity potential saddle points, unstable

--Small fuel requirements for station keeping

L4, L5:

--Local gravitational potential maxima, stable





# Libration Point Use

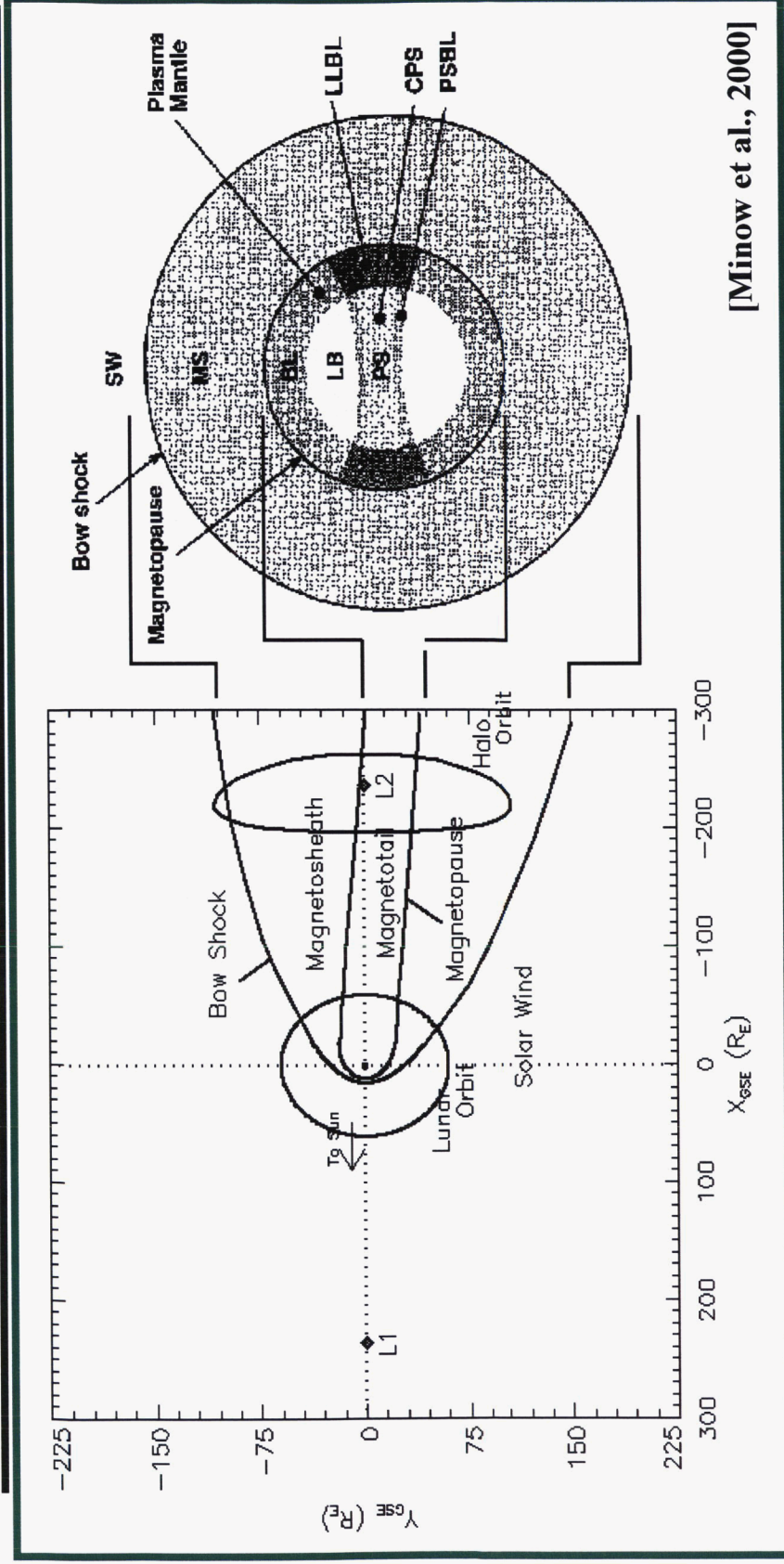
Spacecraft Agency	Location	Mission	Status
• ISEE-3 1978, 1983	NASA	L1,L2	plasma, particles 1992
• Geotail	JAXA/NASA	L2	plasma, particles 1995, 1997
• WIND	NASA	L1,L2	plasma, particles 1996
• SOHO	ESA/NASA	L1	plasma, particles, UV/EUV 1997
• ACE	NASA	L1	plasma, particles 2001
• WMAP	NASA	L2	cosmic microwave background 2001
• Genesis	NASA	L2	solar wind composition 2001
• Spitzer	NASA	L5*	infrared astronomy 2003
• Triana	NASA	L1	plasma, particles, UV/EUV uncertain
• Stereo	NASA	L4, L5**	plasma, particles, UV/EUV 2006
• Herschel	ESA	L2	far infrared telescope 2007
• Planck	ESA	L2	cosmic microwaves background 2007
• Eddington	ESA	L2	stellar observations uncertain
• SIM	NASA	L5*	planet finder (interferometer) uncertain
• LISA Pathfinder	ESA	L1	multi-spacecraft technology demo 2009
• JWST	NASA/ESA	L2	infrared telescope 2013
• Constellation-X	NASA	L2	x-ray astronomy 2012
• GAIA	ESA	L2	galactic structure, astrometry 2011
• DARWIN	ESA	L2	planet finder 2015
• TPF	NASA	L2	planet finder (mid-IR, vis) 2014
• LISA	NASA/ESA	L5*	gravity wave detector 2015
• SAFIR	NASA	L2	infrared observatory 2015-2020

\*1 AU drift-away orbit following Earth \*\*1 AU drift-away orbit leading, following Earth

Sources: Farquhar et al., 2000; ESA Science and Technology website (<http://sci.esa.int/>), NASA (<http://nasa.gov/>)

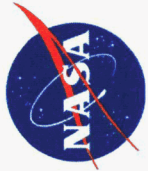


# Plasma Environments

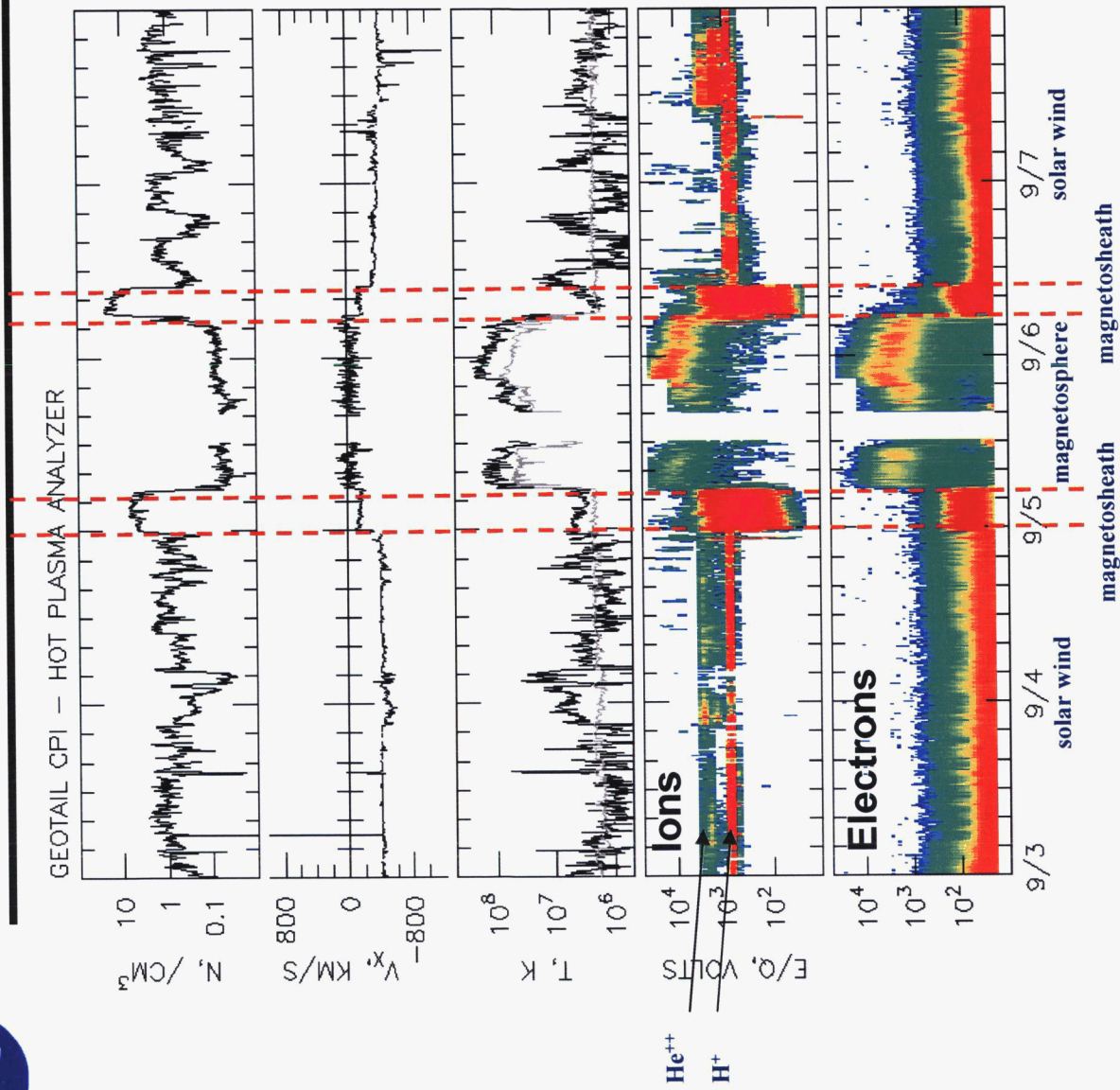


[Minow et al., 2000]

- Sun-Earth L1, L3, L4, L5 all in solar wind
- Sun-Earth L2 located nominally near edge of magnetotail with magnetosheath encounters, solar wind is rare
- Earth-Moon L1, L2, ..., L5 all pass through the magnetosheath and magnetotail once a month but spend most time (~75% in solar wind)

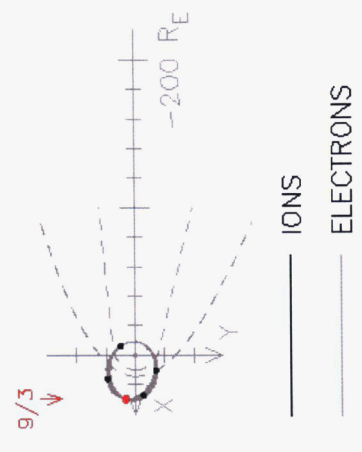


# Plasma Regime Identification

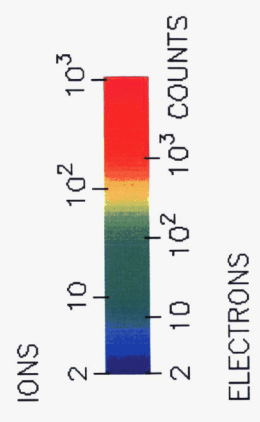


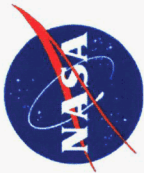
GEOTAIL GPI - HOT PLASMA ANALYZER

3 SEPTEMBER through  
7 SEPTEMBER 1999



Near Earth plasma regimes are well ordered at low energies  
Relatively easy to identify bow shock and magnetopause, plasma regimes by plasma characteristics

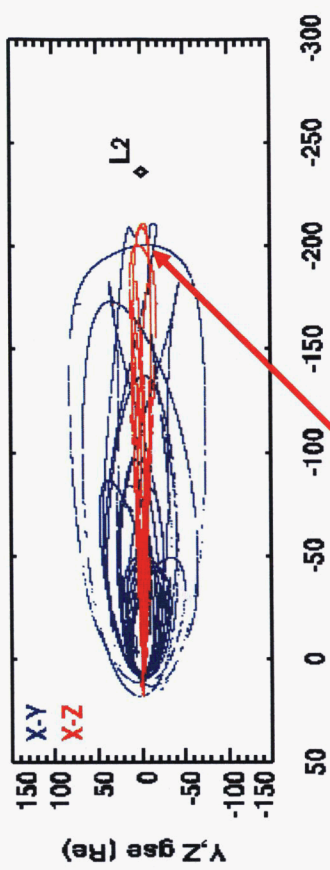




# Distant Magnetotail Environments

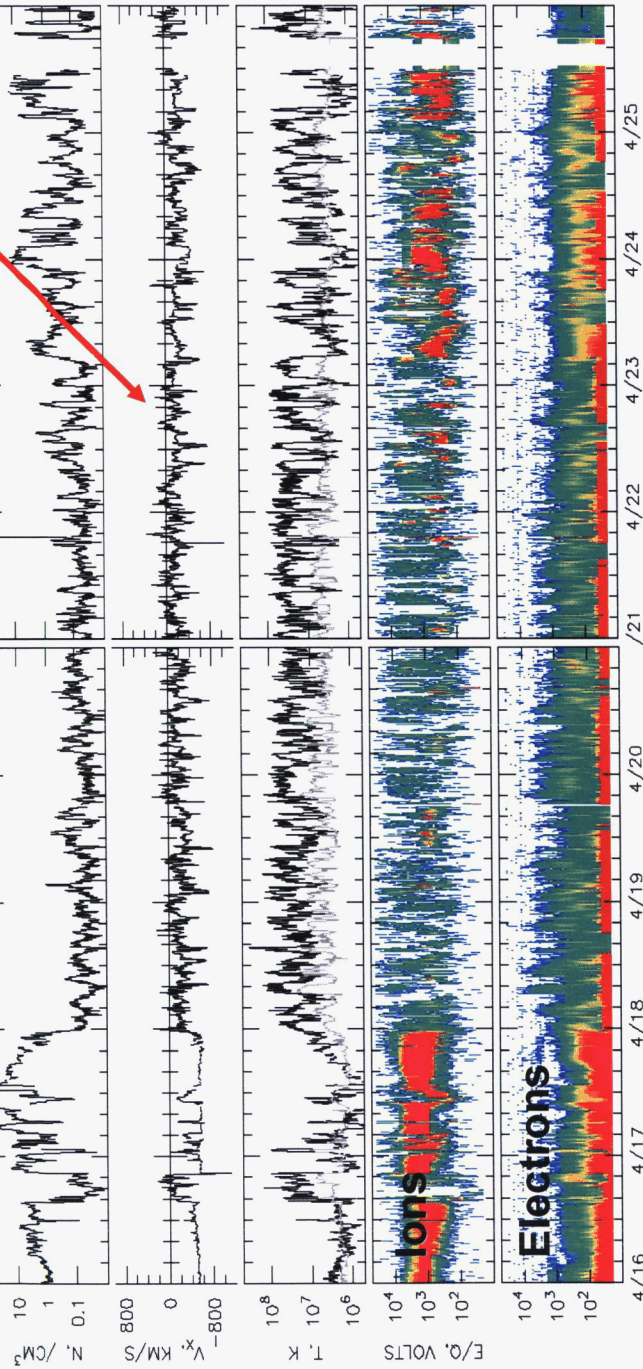
Identification of distant magnetotail plasma regimes is a challenge but plasma properties can be used to characterize plasma regimes into solar wind, magnetosheath, plasma mantle, boundary layer, and plasma sheet.

L2-CPE Database



16-25 April 1994

Geotail CPI/HPA Univ. of Iowa



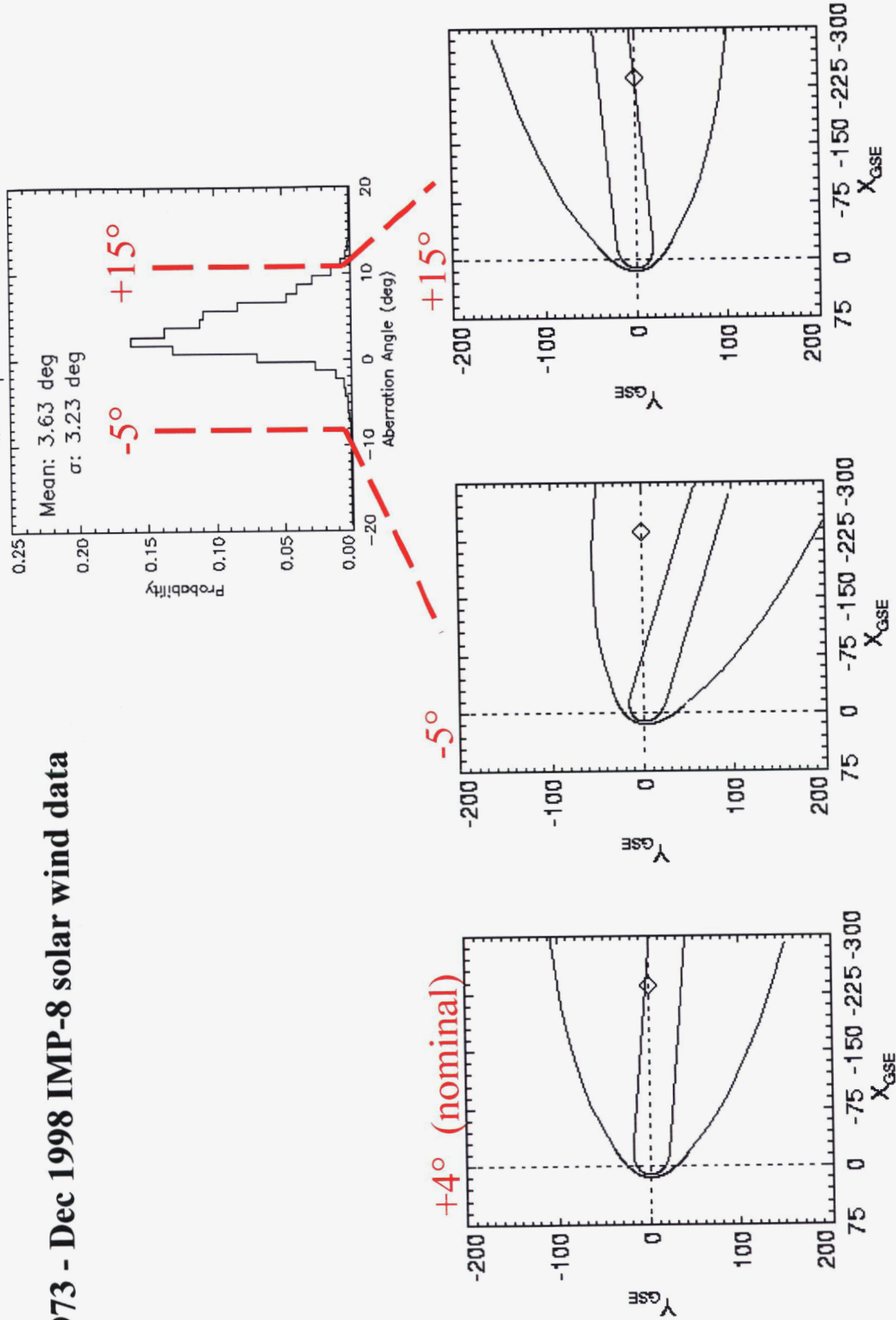
$X_{GSE} \sim -200 \text{ Re}$      $25 \text{ RE} > Y_{GSE} > 0 \text{ Re}$



# Magnetotail Aberration

Magnetotail Aberration  
in Ecliptic Plane

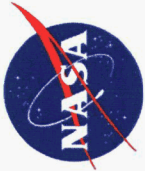
Nov 1973 - Dec 1998 IMP-8 solar wind data



[Blackwell et al., 2000]

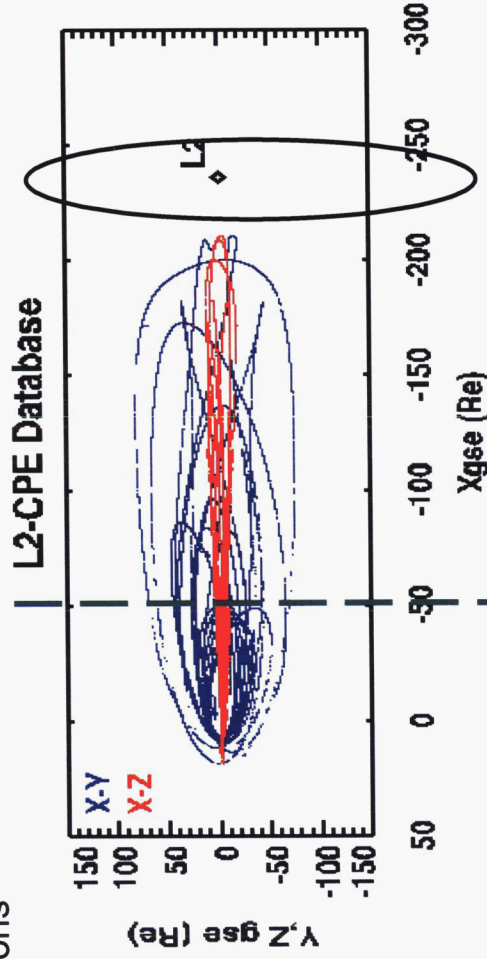
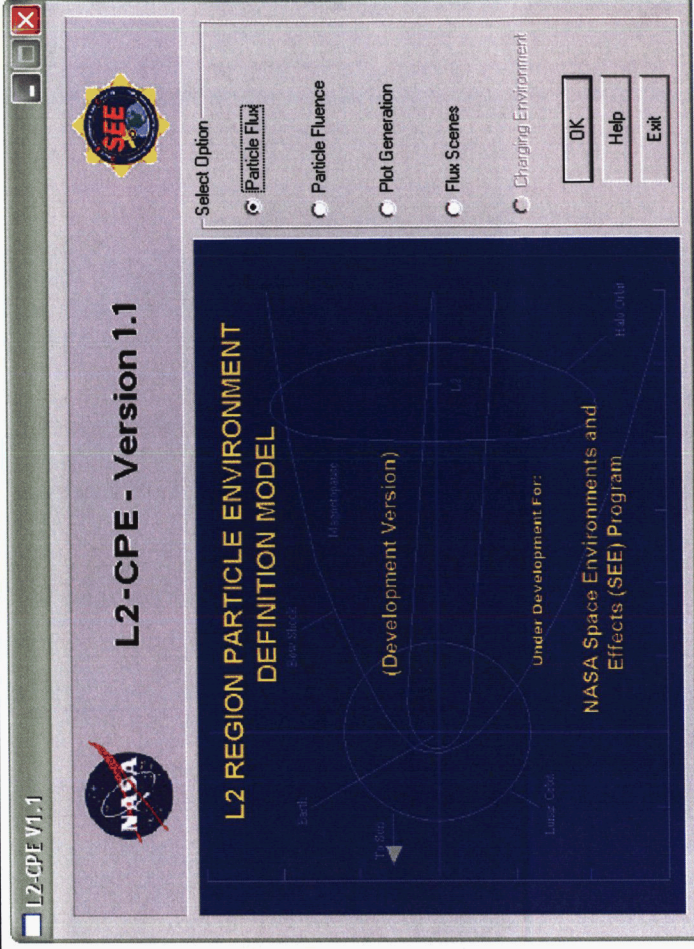
AIAA ASM 2006

Reno, NV January 2007



# L2-Charged Particle Environment Model

- L2 free field plasma environments engineering model
- Limits:
  - $300 R_E < X_{GSE} < 300 R_E$
  - $\sim 0.1 \text{ keV} < E < \sim 1 \text{ MeV}$
- Based on in-situ satellite measurements of plasma properties ( $< 1 \text{ MeV}$ ) in solar wind and distant magnetotail plasma regimes
- Solar wind, magnetosheath, and magnetotail plasma environments ordered by solar wind dependent bow shock and magnetopause boundaries
- Empirical model flux, fluence output traceable to observations



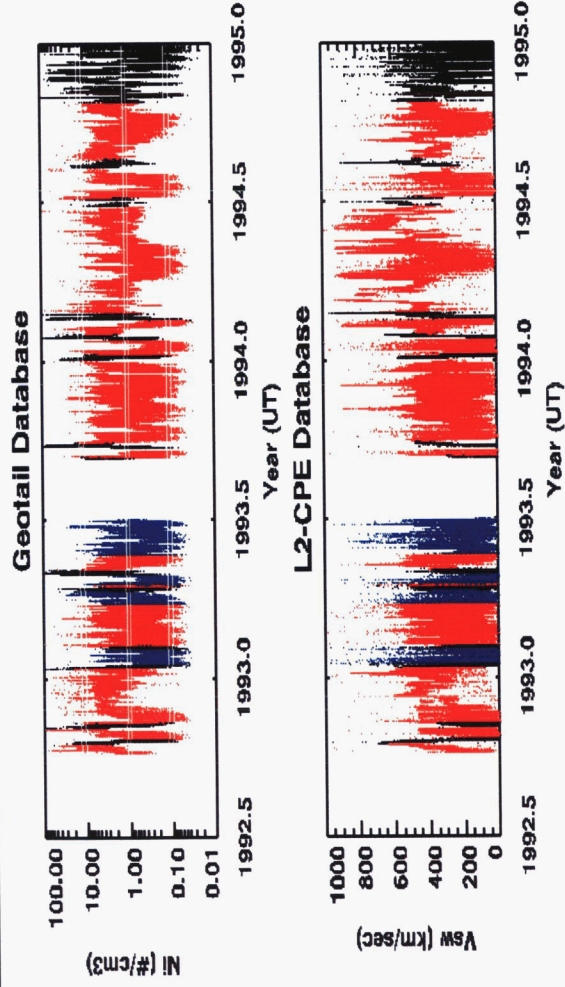
**L2-CPE includes complete  
2+ years Geotail distant  
magnetotail records**



# Databases, Orbit Propagation

L2-CPE Plasma	
Database Records	
Solar Wind	
--IMP 8 solar max	105,120 ( $\Delta t = 10$ min)
--IMP8 solar min	105,120 ( $\Delta t = 10$ min)
--Ulysses solar max	32,342 ( $\Delta t = 60$ min)
--Ulysses solar min	25,106 ( $\Delta t = 60$ min)
Magnetosheath	
--Geotail	212,426 ( $\Delta t = 10$ min)
Plasma mantle	
--Geotail	99,420 ( $\Delta t = 10$ min)
Plasma sheet	
--Geotail	71,752 ( $\Delta t = 10$ min)

- **Halo orbit generator**
  - Analytical halo orbits [Farquhar, 1970; Richardson, 1980] convenient method for conducting trades
- **User provided ephemerides**
  - Lissajous orbits about L2, trajectory to and/or from L2, and other trajectories treated with user provided ephemeris
- **L2-CPE is a two-dimensional model**
  - $Y_{GSE}$ ,  $Z_{GSE}$  position determines if spacecraft is in the solar wind, magnetosheath, or magnetotail
  - No  $X_{GSE}$  variation in plasma environments
  - L2-CPE is applicable for  $-300 R_E \leq X_{GSE} \leq -100 R_E$ 
    - Geotail data from  $X_{GSE} \leq -50 R_E$  is included in the database due to sparseness of the data



All Geotail  
 LRAD  
 LRAD + L2-CPE

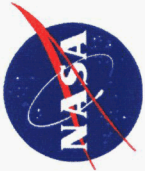
Remaining records in black are  $>50 R_E$  from Earth and not used in L2-CPE





# Data Sources

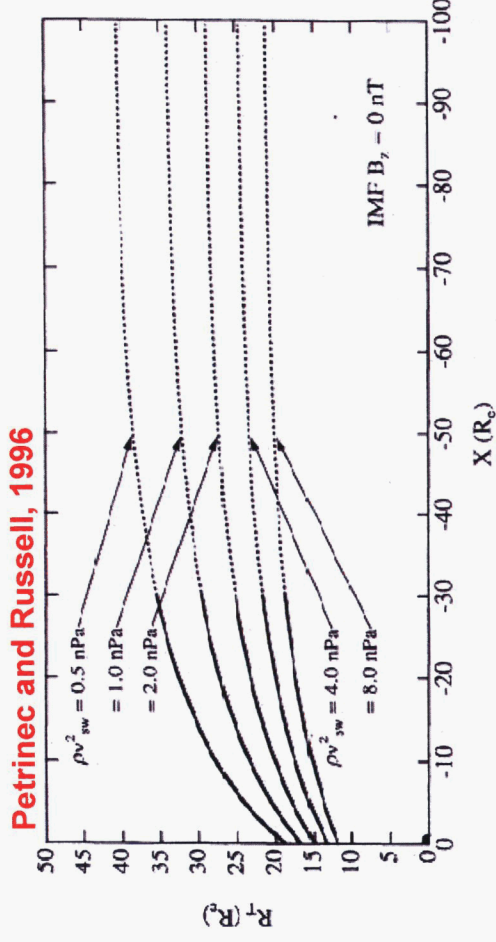
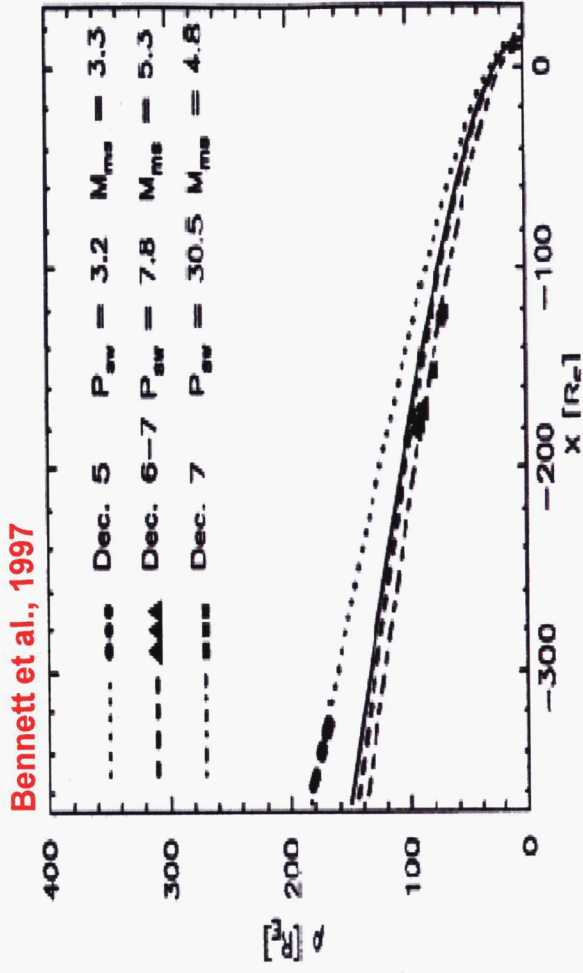
Spacecraft/Instrument	Application	Source
<b>Geotail</b> <b>10 Re x 210 Re, near ecliptic</b> --Comprehensive Plasma Instrument/Hot Plasma Analyzer (CPI/HPA) --Energetic Particle and Ion Composition/Ion Composition Subsystem (EPIC/ICS) --Geotail plasma regime identification	<b>Magnetotail, magnetosheath</b>  core plasma moments  non-thermal ion, electron flux  database organization	Univ. of Iowa  JHU/APL (ions) NSSDC/JHU/APL (electrons) EPIC Science Team, JHU/APL
<b>IMP-8</b> <b>~35 Re circular, near ecliptic</b> --MIT Faraday Cup --Magnetic Field Experiment --Charged Particle Measuring Experiment (CPME) --Energetic Particle Experiment (EPE)	<b>Solar wind</b>  core plasma moments interplanetary magnetic field non-thermal ion, electron (not implemented) non-thermal ion, electron (not implemented)	MIT NSSDC (GSFC) JHU/APL JHU/APL
<b>Ulysses</b> <b>1 to 5.5 AU, 1.3 AU x 5.4 AU, 78°</b> --Solar Wind Observations Over the Poles of the Sun (SWOOPS) --Low Energy Magnetic Spectrometer (LEMS) --Low Energy Foil Spectrometer (LEFS)	<b>Solar wind</b>  core/halo electron, core ion plasma moments  non-thermal ion, electron flux non-thermal ion, electron flux	NSSDC/SwRI  NSSDC/Lucent Technologies NSSDC/Lucent Technologies



# Bow Shock, Magnetopause Models

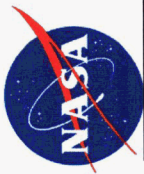
Bennett et al., 1997 bow shock model

- Model applicable for bow shock from subsolar point to  $-400 R_E < X_{GSE}$
- Note bow shock radius at L2 distance of  $\sim 236 R_E$  is  $\sim 120 R_E$ .



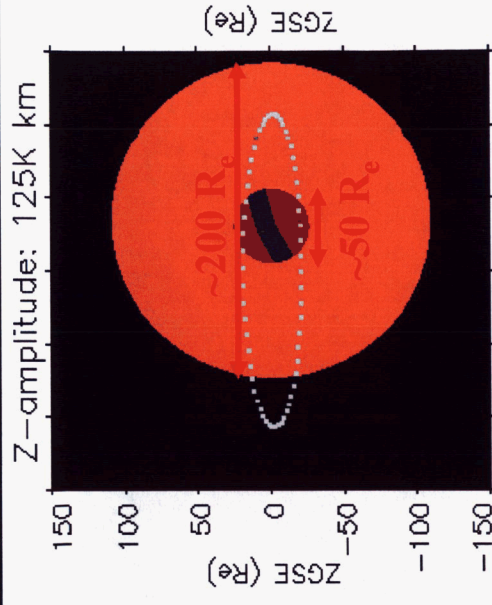
Petrinec and Russell [1996]

- magnetopause Model validated for  $-30 R_E < X_{GSE}$  but extrapolated to greater distances
- Extrapolation to L2 distances used in L2-CPE based on information from ISEE-3, Geotail spacecraft magnetopause encounters



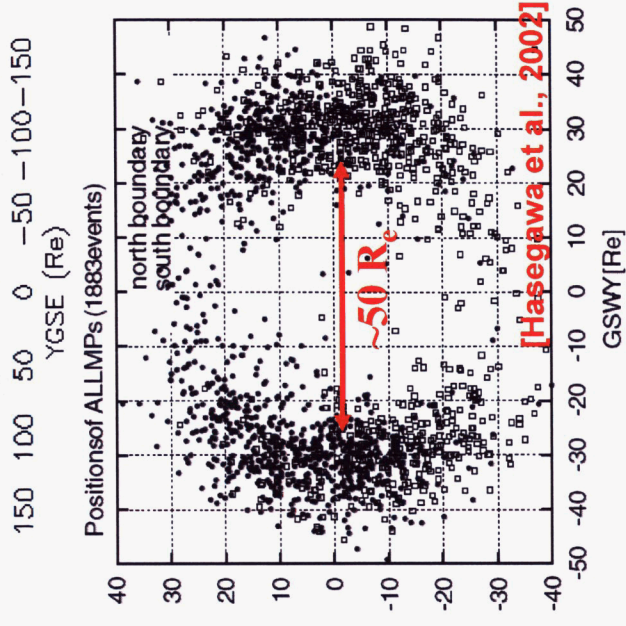
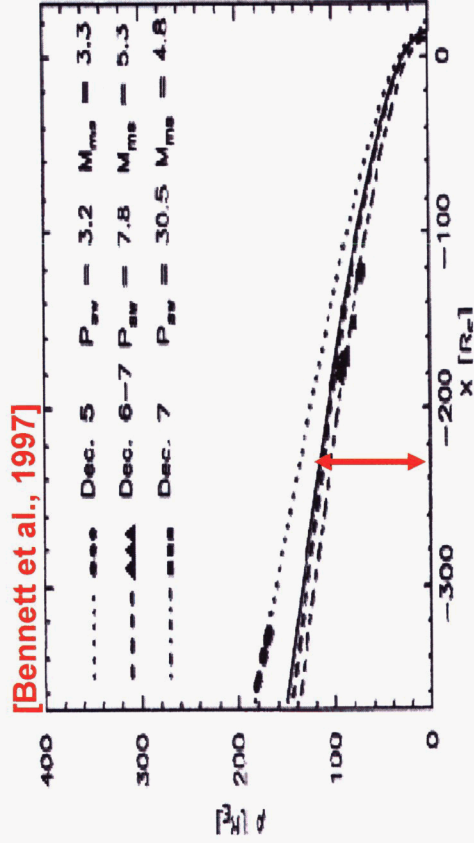
# Distant Magnetotail Boundaries

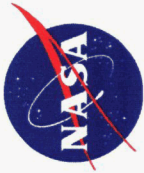
Extrapolated *Petrinec and Russell [1996]* magnetopause and *Bennett et al. [1997]* bow shock boundaries consistent with Geotail, ISEE-3 magnetopause encounters reported in the literature including *Sibeck et al. [1986]*, *Fairfield [1992]*, *Christon et al. [1998]*, *Maenzawa and Hori [1998]*, *Hasegawa et al. [2002]* and the numerous references included *Lui [1987]* and *Nishida et al. [1998]*.



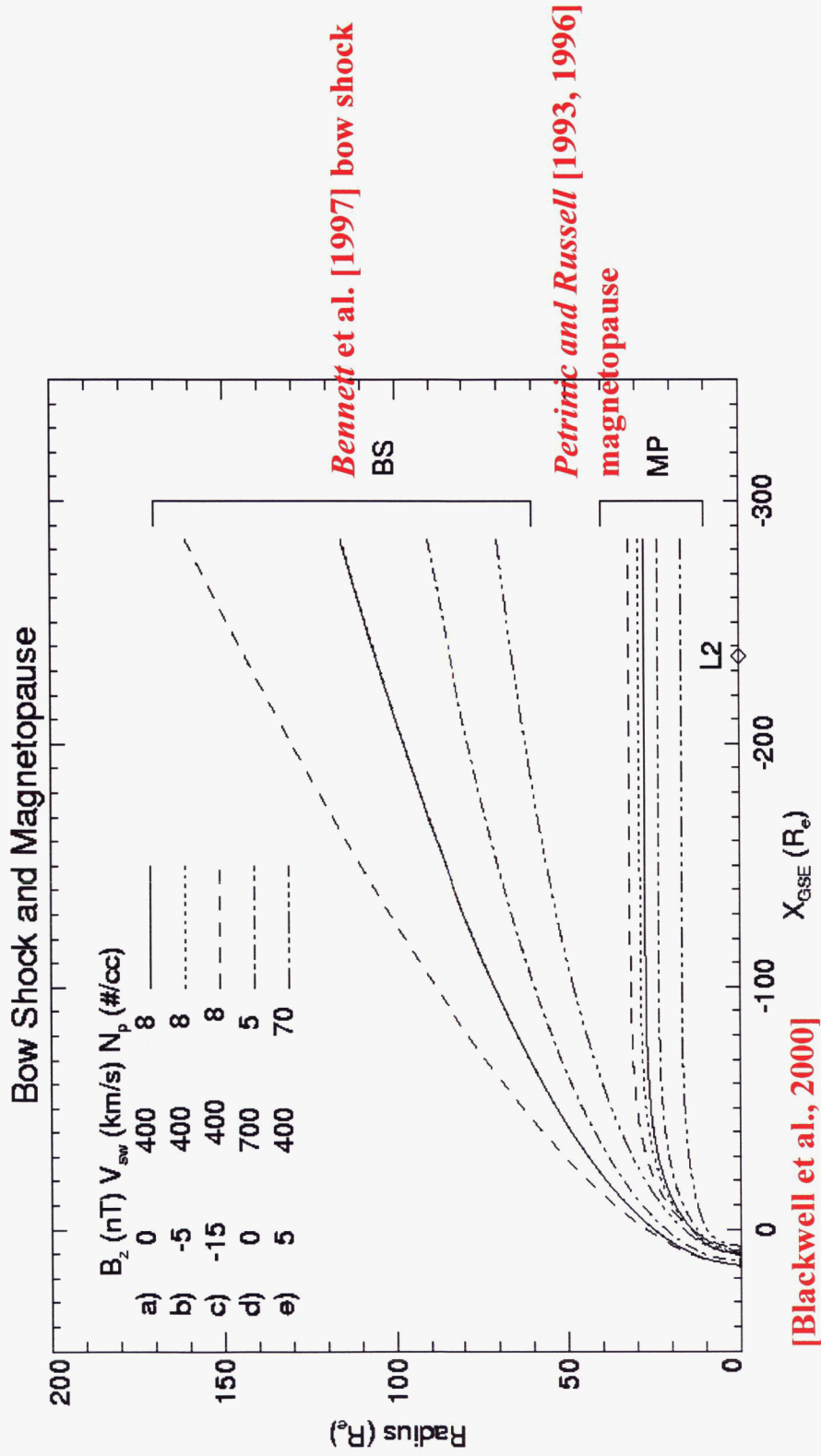
## Examples:

- *Hasegawa et al. [2002]* Geotail magnetopause encounters from  $-210 R_E \leq X_{GSE} \leq -100 R_E$  consistent with L2-CPE
- *Bennett et al. [1997]* bow shock radius at L2 consistent with L2-CPE model





# Bow Shock and Magnetopause Variability



**IMP-8 plasma parameters with mean Parker spiral orientation for IMF provide variations in bow shock, magnetopause orientation and dimensions**



# Ulysses Differential Flux Reconstruction

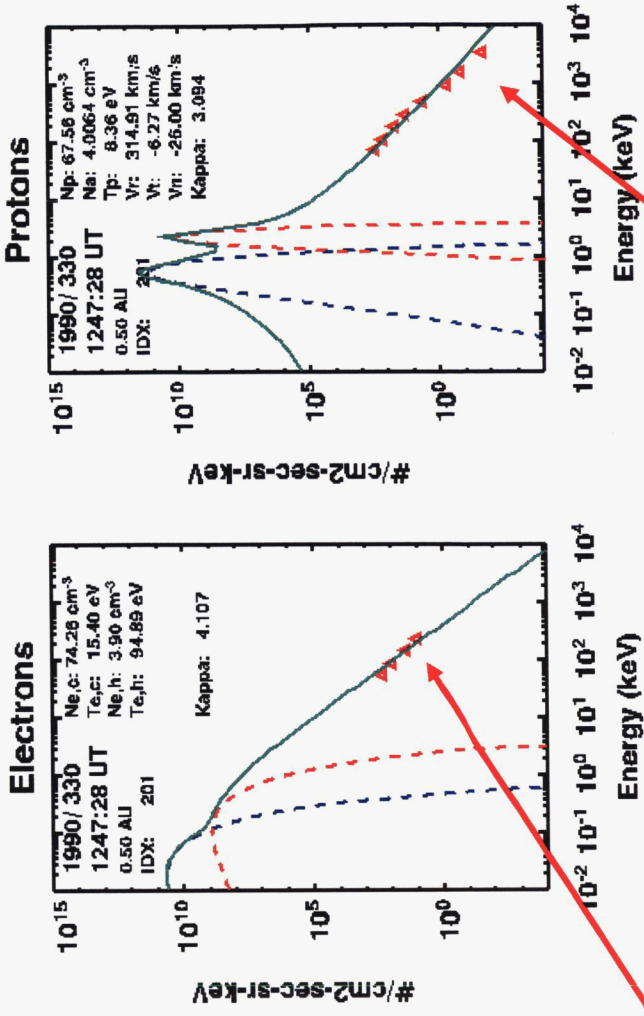
## Maxwellian differential flux distributions

$$f(\mathbf{v}) = \frac{n_0}{(\sqrt{\pi}\theta_{MB})^3} \exp\left[-\frac{(\mathbf{v}-\mathbf{u})^2}{\theta_{MB}^2}\right] \theta_{MB} = \sqrt{\frac{2k_B T_i}{m_i}}$$

## Kappa differential flux distributions

$$f(v) = \frac{n_0}{(\sqrt{\pi}\theta_\kappa)^3} \frac{\Gamma(\kappa+1)}{\sqrt{\kappa^3}\Gamma(\kappa-\frac{1}{2})} \left[1 + \frac{v^2}{\kappa\theta_\kappa^2}\right]^{-\kappa-1}$$

$$\theta_\kappa = \sqrt{\frac{(2\kappa-3)k_B T}{\kappa m}}, \quad \kappa > \frac{3}{2}$$



**LEMS, LEFS electrons**

**LEMS, LEFS protons**

- Ulysses Solar Wind Over the Poles of the Sun (SWOOPS) plasma moments provide low energy environments
- $\kappa$  parameter constrained by matching Low Energy Magnetic Spectrometer (LEMS), Low Energy Foil Spectrometer (LEFS) differential flux measurements
- LEMS (LEFS) at 30°, 120° (60°, 150°) from Ulysses spin axis



# Geotail Differential Flux Reconstruction

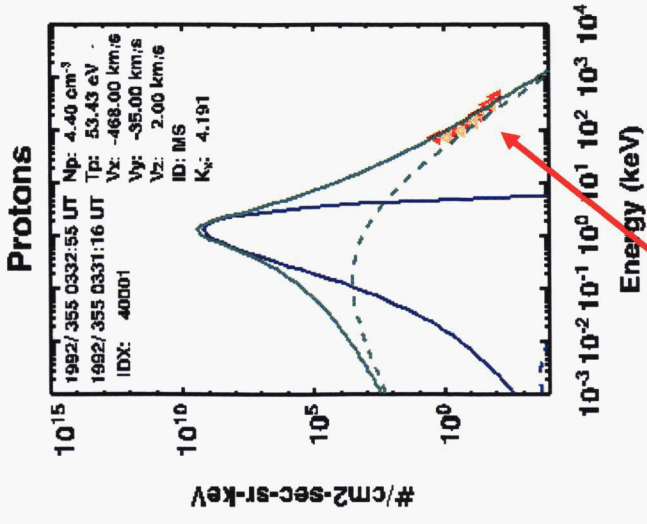
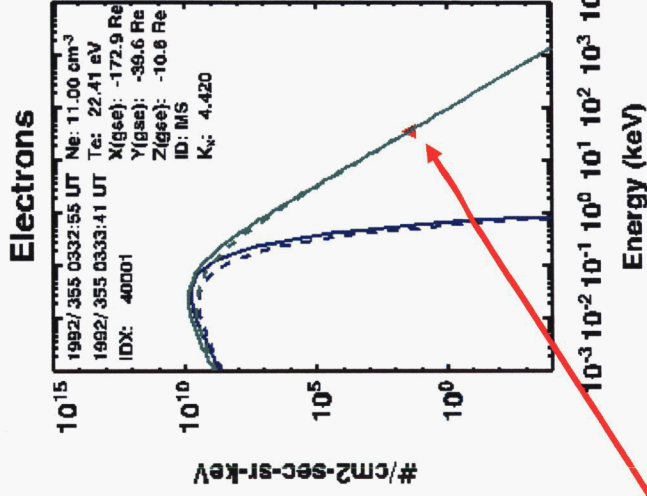
## Maxwellian differential flux distributions

$$f(\mathbf{v}) = \frac{n_o}{(\sqrt{\pi}\theta_{MB})^3} \exp\left[-\frac{(\mathbf{v}-\mathbf{u})^2}{\theta_{MB}^2}\right] \theta_{MB} = \sqrt{\frac{2k_B T_i}{m_i}}$$

## Kappa differential flux distributions

$$f(\mathbf{v}) = \frac{n_o}{(\sqrt{\pi}\theta_\kappa)^3} \frac{\Gamma(\kappa+1)}{\sqrt{\kappa^3}\Gamma(\kappa-\frac{1}{2})} \left[1 + \frac{v^2}{\kappa\theta_\kappa^2}\right]^{-\kappa-1}$$

$$\theta_\kappa = \sqrt{\frac{(2\kappa-3)k_B T}{\kappa m}}, \quad \kappa > \frac{3}{2}$$



**EPIC E>38 keV electrons**

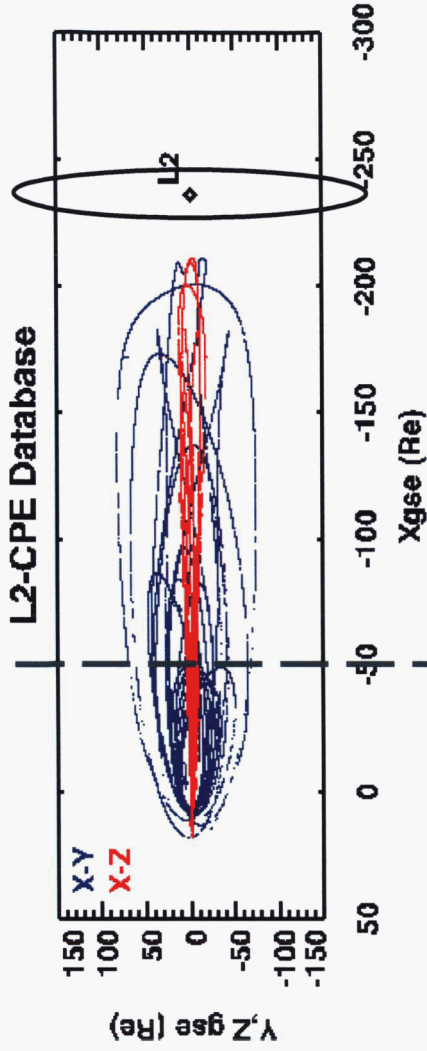
**EPIC/ICS protons**

- Geotail Comprehensive Plasma Instrument (CPI) Hot Plasma Analyzer (HPA) plasma moments provide low energy environments
- $\kappa$  parameter constrained by matching Energetic Particle and Ion Composition (EPIC) Ion Composition Subsystem (ICS) differential ion flux, integral electron flux measurements
- Ions in 16 azimuths, electrons are spin averaged



# Sparse Data

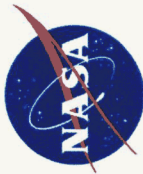
- L2-CPE uses all 2+ years Geotail records appropriate for distant magnetotail
  - Database is still sparse!
- All Geotail magnetosheath, plasma mantle, boundary layer, lobe, and plasma sheet records beyond -50 Re are used in database
  - Source of plasma in distant magnetotail is solar wind mirroring in plasma mantle and local entry beyond ~ -50 Re [Baker and Pulkkinen, 1998]
- Plasma mantle, boundary layer, lobe are combined in a single "plasma mantle" environment
- Insufficient Geotail solar wind records to provide good statistics
  - Solar wind environment provided by IMP-8, Ulysses data sets which also drive the magnetotail



Data with  $X_{GSE} < -50 Re$  used in models

- Insufficient records to model spatial variations of plasma environments as function of distance from Earth-Sun line within plasma regimes
- Insufficient records to model  $X_{GSE}$  variations of plasma regimes
- **No spatial variations within the individual plasma**
- **--Halo, Lissajous orbits about L2 are not represented by the Geotail orbit**
- **--Integrating Geotail environments along the Geotail orbit would not provide a good representation of particle fluences accumulated while in orbit about L2**
- **--L2-CPE utilizes a technique of random sampling the Geotail records to model environments which vary in time and space**

**--Statistics of environment variations are constrained by the data base**



# EPIC Science Team Region Identifications

- EPIC Science Team plasma regime identifications (RID) for 1 Oct 1992 through 31 Oct 1994 [Eastman et al., 1998; Christon et al., 1998] are adopted for L2-CPE
- Geotail records (CPI/HPA moments, EPIC flux) time tags compared to regime identification file to determine into which plasma regime database (SW, MS, PM, or PS) to place the record in the model

Geotail Regime IDs for: 94-106 0000 to 94-115 0000

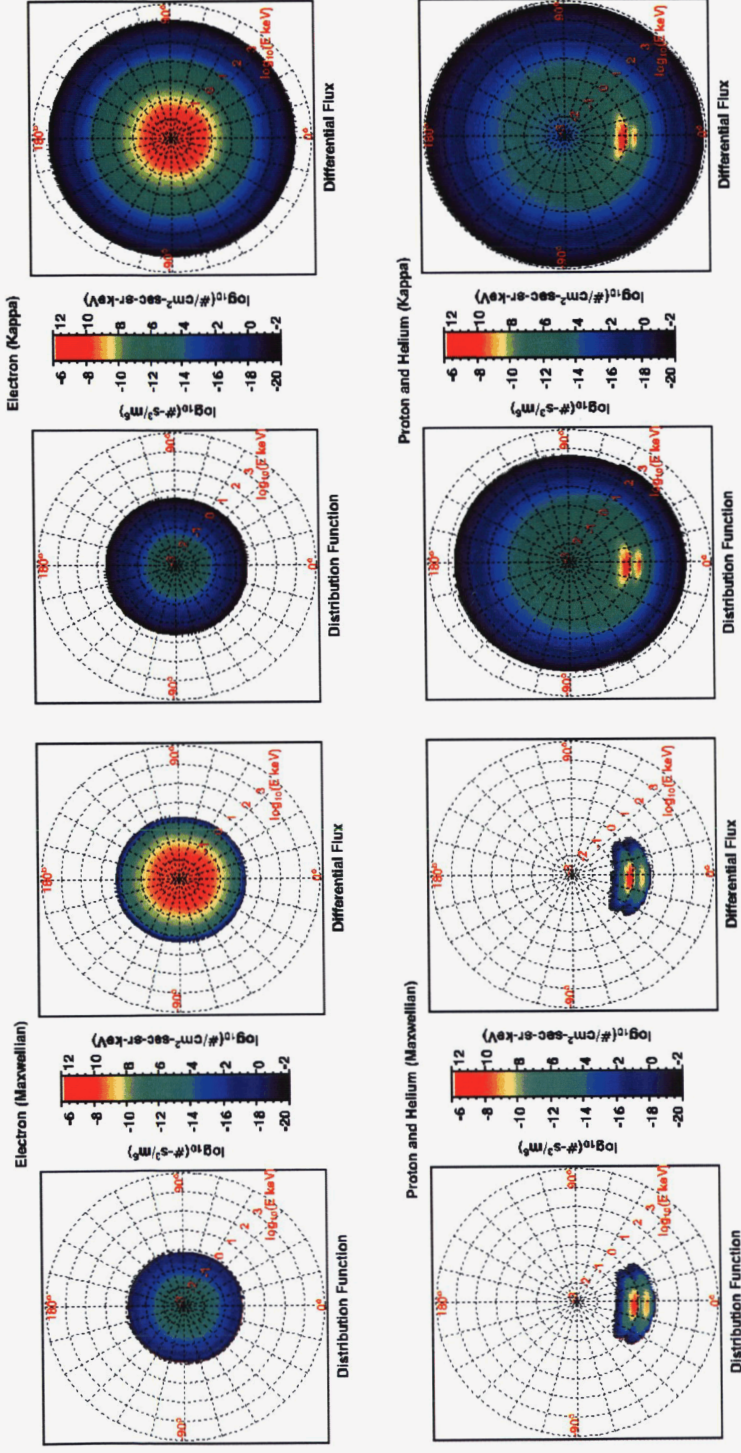
Start Date/Time	End Date/Time	Interval minute	min	avg	max	X	Y	Z	Stop_Pos_ (GSE Re)	X	Y	Z	Region =	##	Notes
94-105 2016	- 94-106 0805	709	2.7	3.5	3.7	-196.6	28.0	-5.1	-196.8	26.8	-4.7	MS = 44			
94-106 0805	- 94-106 0814	9	3.3	3.3	3.3	-196.8	26.8	-4.7	-196.8	26.8	-4.7	BL/MS = 34			
94-106 0814	- 94-106 0928	74	2.3	2.8	3.3	-196.8	26.8	-4.7	-196.9	26.7	-4.7	MS = 44			LEP Data gap: 0140-0142
94-106 0928	- 94-106 0940	12	2.3	2.3	2.3	-196.9	26.7	-4.7	-196.9	26.7	-4.7	MS/BL = 43			
94-106 0940	- 94-106 1146	126	2.3	2.3	2.3	-196.9	26.7	-4.7	-196.9	26.5	-4.6	MS = 44			
94-106 1146	- 94-106 1156	10	2.3	2.3	2.3	-196.9	26.5	-4.6	-196.9	26.4	-4.6	PS = 11			
94-106 1157	- 94-106 1519	202	2.3	2.9	3.3	-196.9	26.4	-4.6	-197.0	26.1	-4.5	MS = 44			LEP Data gap: 1245-1251
94-106 1520	- 94-106 1531	11	3.3	3.3	3.3	-197.0	26.1	-4.5	-197.0	26.1	-4.5	PS = 11			PSBL after 1528
94-106 1532	- 94-106 1551	19	3.3	3.3	3.3	-197.0	26.1	-4.5	-197.0	26.1	-4.5	BL = 33			
94-106 1552	- 94-106 1611	19	3.3	3.3	3.3	-197.0	26.1	-4.5	-197.0	26.0	-4.5	PS = 11			

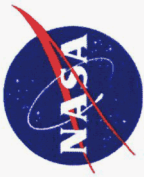




# Kappa Flux Reconstruction Process

1. Compute Kappa distribution functions from plasma moments, initial guess for  $\kappa$  parameter
2. Differential flux is computed from distribution functions using the relationship  $J = p^2 f$
3. Differential flux at energies of 10's to 100's keV is compared to flux measurements
4. If measured and computed flux is not within specified error tolerance, value of  $\kappa$  parameter is adjusted and steps 1 to 3 are repeated. The iterative process is used to obtain a  $\kappa$  parameter which gives the best differential flux based on comparison with measured differential flux





# L2-CPE Halo Orbit Fluence (10 years)

## Max. proton flux

Mean:  $0.216 \times 10^{17}$  #/cm<sup>2</sup>

95%:  $0.240 \times 10^{17}$  #/cm<sup>2</sup>

Max:  $0.265 \times 10^{17}$  #/cm<sup>2</sup>

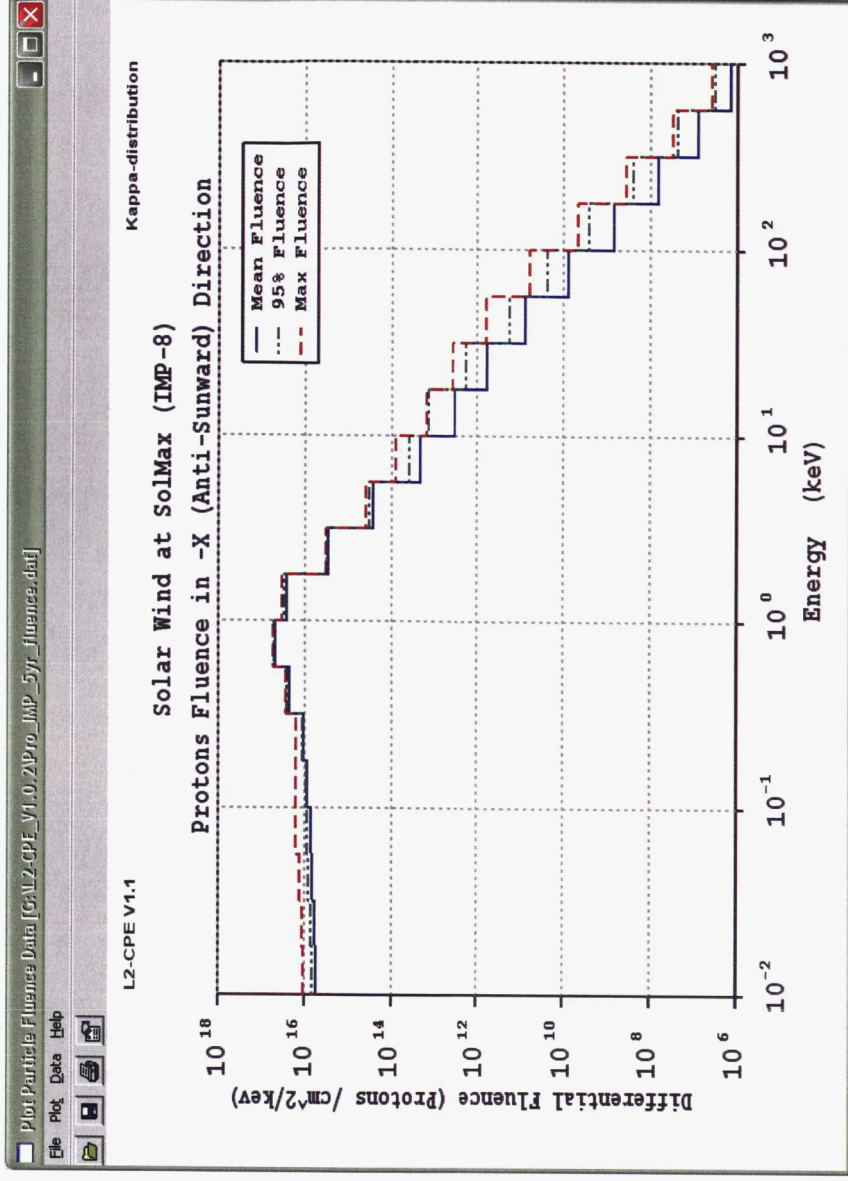
Maximum environment is a credible worst case environment because it is the largest fluence derived from integrating real flux measurements in the database

5% chance that the 95% fluence will be exceeded for a given integration period

Compare with solar wind for ten years:

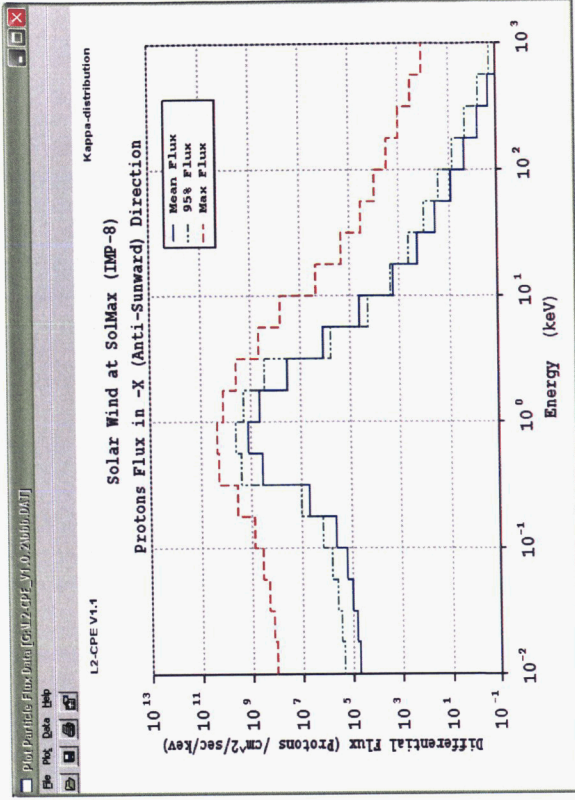
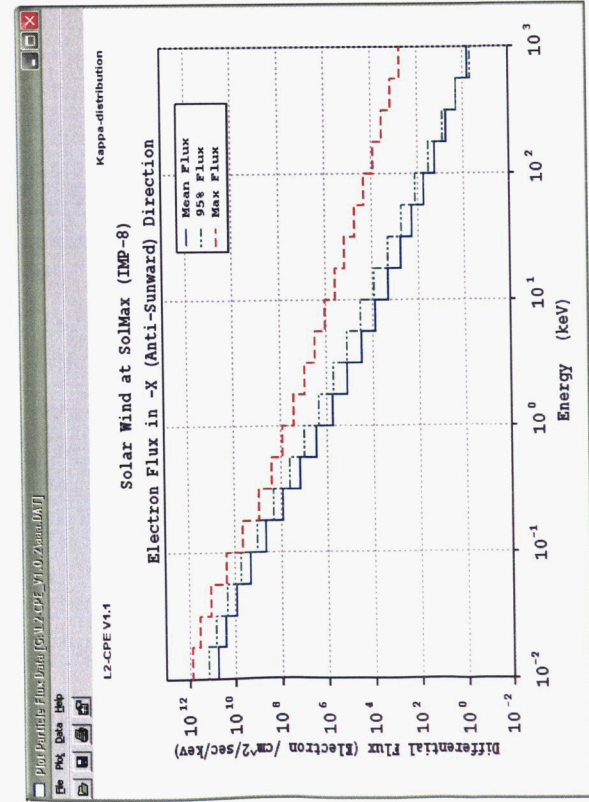
fluence  $\sim (3 \times 10^8 \text{ H}^+/\text{cm}^2\text{-sec})(3 \times 10^7 \text{ sec})(10 \text{ yrs}) = 9 \times 10^{16} \text{ H}^+/\text{cm}^2\text{-sec}$

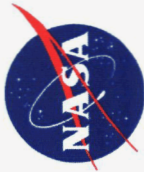
$\sim 10^{17} \text{ H}^+/\text{cm}^2\text{-sec}$



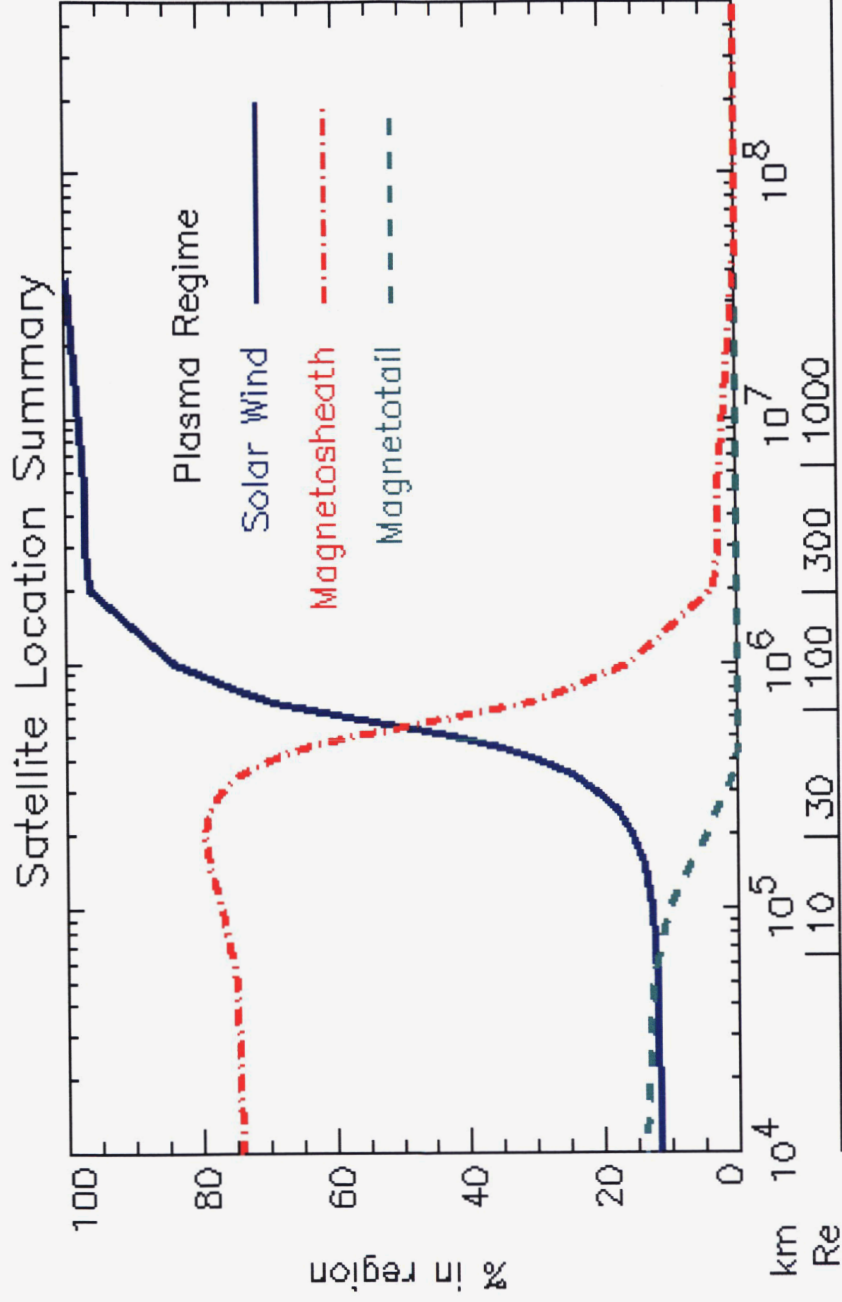


# L2-CPE Solar Wind Flux





# Halo Orbit Size and Plasma Regimes



[Minow et al., 2004]



# Luna - CPE

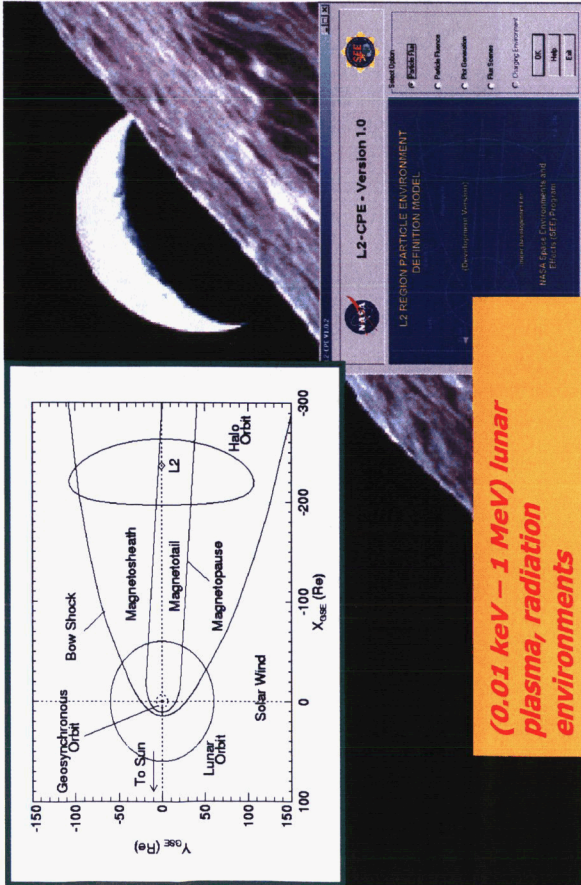
---

- Modifications to L2-CPR funded by SEE Program to include environments relevant to lunar missions
  - Update database (additional Geotail data)
  - Lunar wake
  - Lunar orbits



# Lunar-Charged Particle Environment (Lunar-CPE)

## Space Environments and Effects (SEE) Program



### Description:

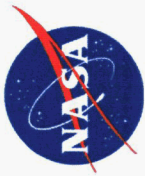
- Update L2-Charged Particle Environment (L2-CPE) model (applicable over  $-100 \text{ Re} < X_{GSE} < -300 \text{ Re}$ ) to include outer magnetosphere ( $>6 \text{ Re}$ ), through lunar ( $60 \text{ RE}$ ), and lunar to  $-100 \text{ Re}$  environments;
- Space plasma ( $0.01 \text{ keV}$  to  $500 \text{ keV}$ ) and low energy ionizing radiation ( $500 \text{ keV}$  to  $10^6 \text{ MeV}$ ) engineering environment model provides ion, electron flux and fluence for spacecraft charging and radiation degradation analysis;
- Model derived from ion, electron flux measurements which provides statistical environments (e.g., percentile electron, ion flux at 50%, 95% level) to support spacecraft design and program decisions on environment risk.

### Benefits to NASA:

- Engineering ion, electron environment model provides flux, fluence spectra for ions, electrons from  $0.1 \text{ keV}$  through  $1 \text{ MeV}$  for use in spacecraft design and mission analysis;
- Graphical user interface provides user friendly access for spacecraft design engineers, radiation health physicists, materials scientists, and space environments analysts to environment data for cis- and trans-lunar missions;
- Leverages L2-CPE funding from NASA's SEE and JWST programs and MSFC/ED44 experience in space plasma and radiation environments support for the Chandra, ISS, and MSFC/Transportation Directorate Solar Sail programs to develop tools for space environments analysis.

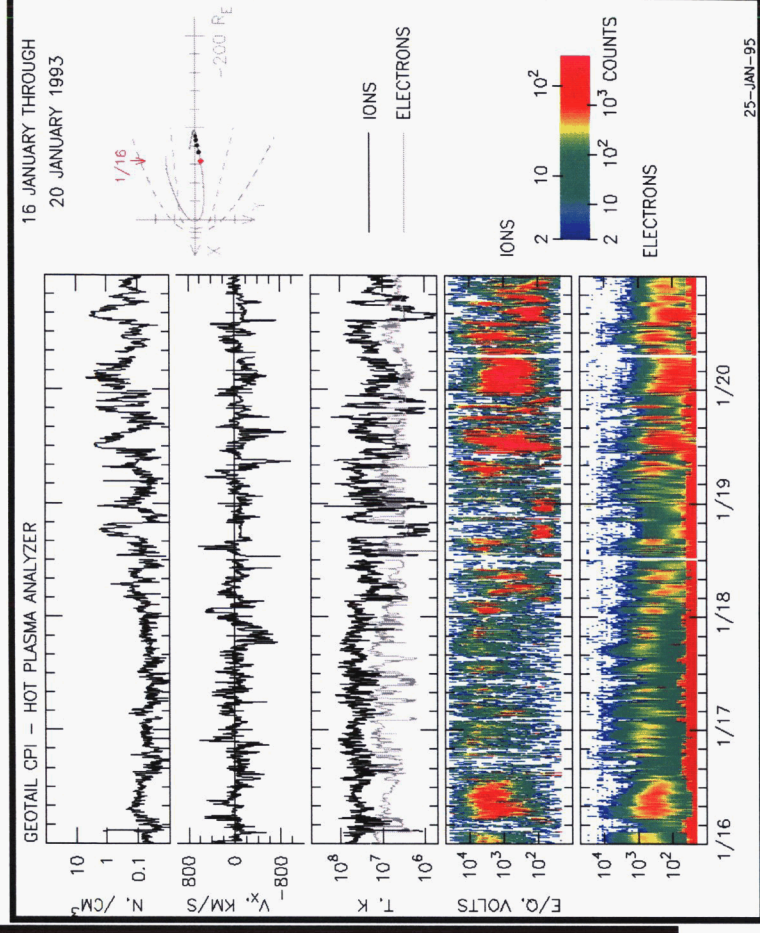
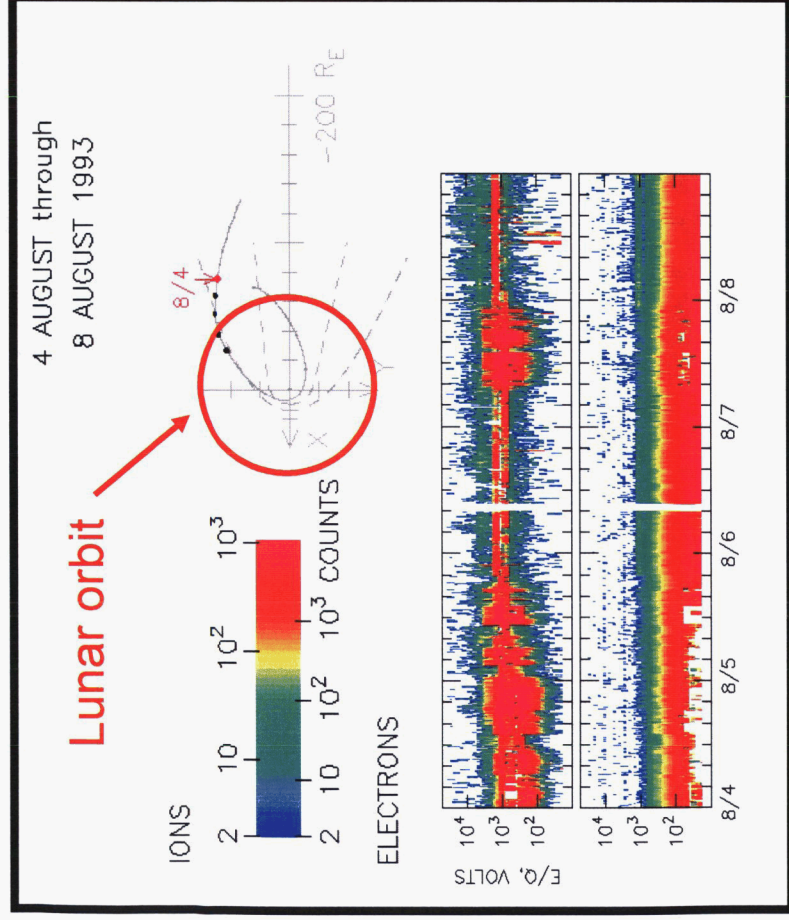
### Schedule & Cost:

<ul style="list-style-type: none"> <li>• Process in-house data and acquire additional electron, ion flux data sets</li> <li>• Modify L2-CPE structure for new data</li> <li>• Incorporate near Earth, cis-lunar magnetotail, magnetosheath, and solar wind data into L2-CPE structure</li> <li>• Release beta-test version of Lunar-CPE</li> </ul>	<p>FY04</p>
<p>AIAA ASIM 2006 Reno, NV January 2007</p>	
<p>23</p>	

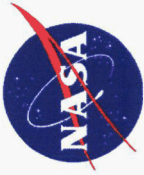


# Magnetotail Plasma at Lunar Distances

- Lunar plasma environment includes encounters with magnetotail and magnetosheath
  - Variability due to solar wind driven motion of magnetotail
- High temperature, low density plasma environments in magnetotail



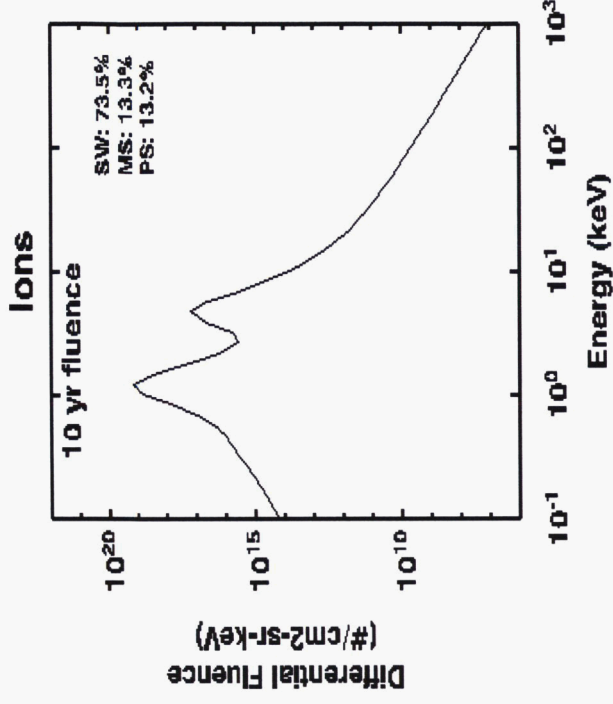
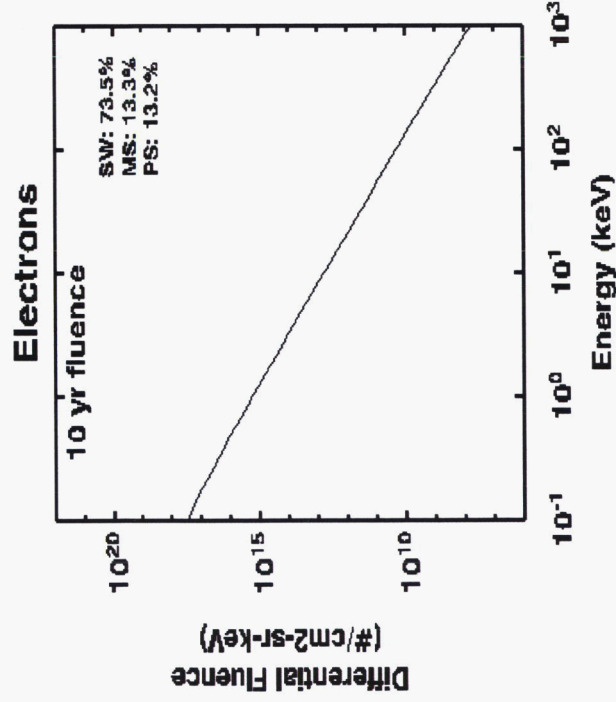
(Univ. of Iowa)



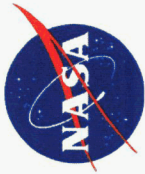
# Free Field Plasma Environments

---

- Moon spends
  - ~73.5% solar wind
  - ~13.3% magnetosheath
  - ~13.2% magnetotail
- Solar wind fluence
  - $\sim(3 \times 10^8 \text{ protons/cm}^2\text{-sec})(3 \times 10^7 \text{ sec/yr})$
  - $\sim 9 \times 10^{15} \text{ protons/cm}^2$



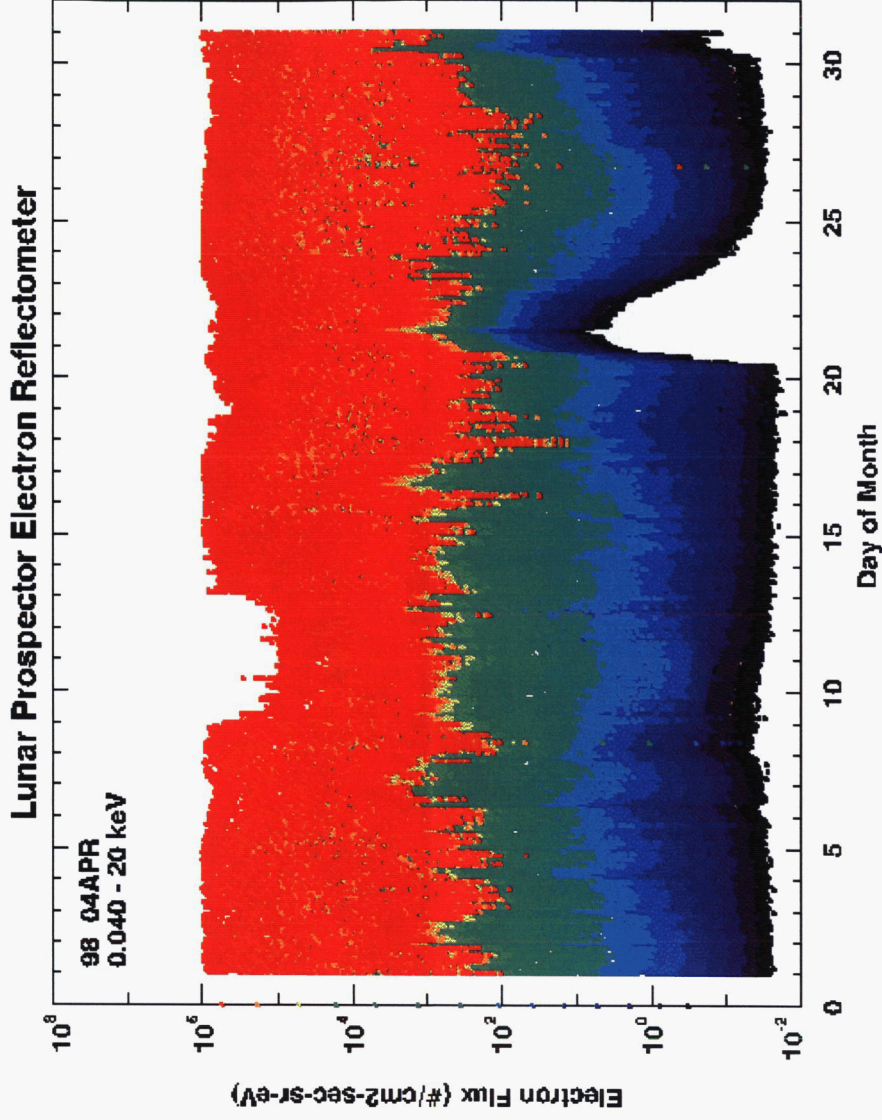


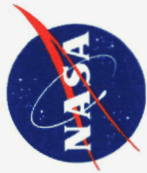


# Lunar Plasma Environments

---

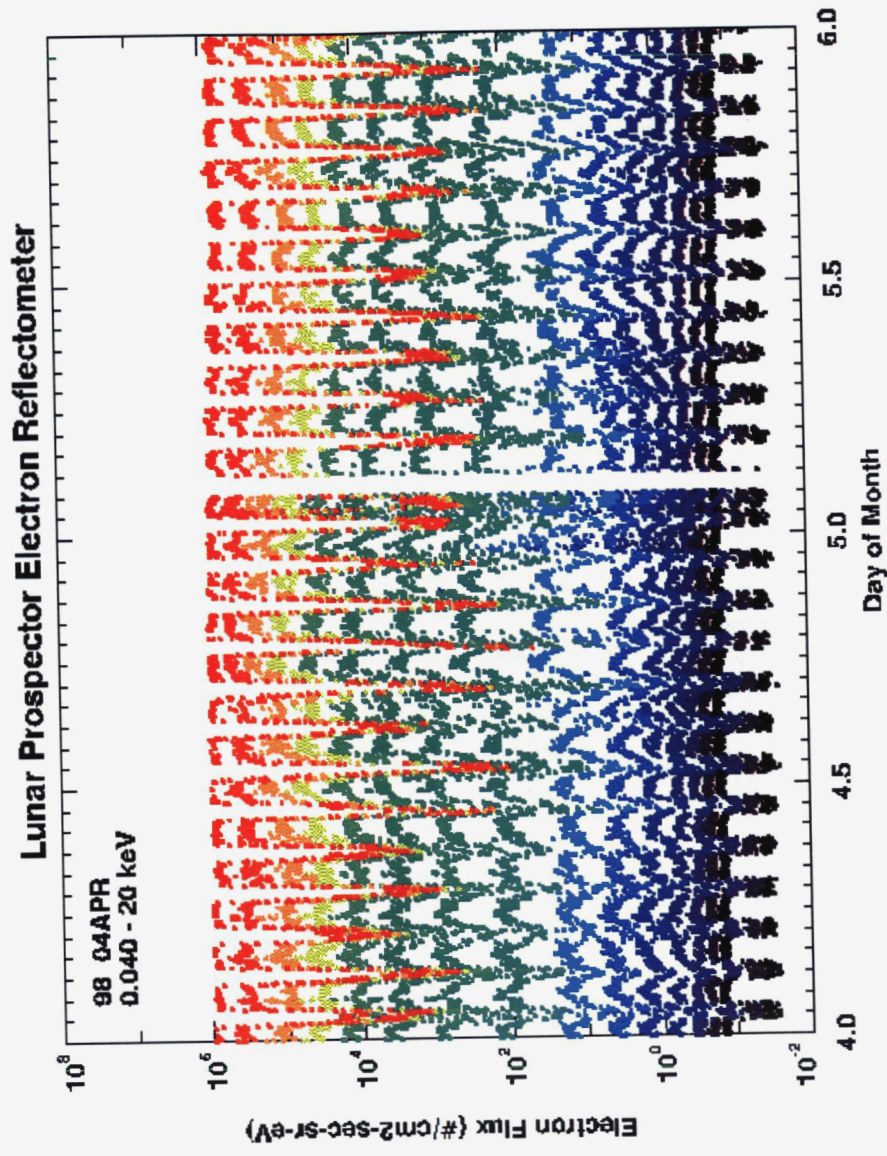
- Lunar Prospector Electron Reflectometer
  - Spin average electron flux
  - ~40 eV to ~20 keV
- April 1998
  - Earth's magnetotail
  - Solar energetic particle event

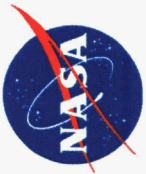




# Lunar Plasma Environments

- Lunar Prospector Electron Reflectometer
  - Spin average electron flux
  - ~40 eV to ~20 keV
- 4-5 April 1998
  - Moon in solar wind
  - Plasma wake

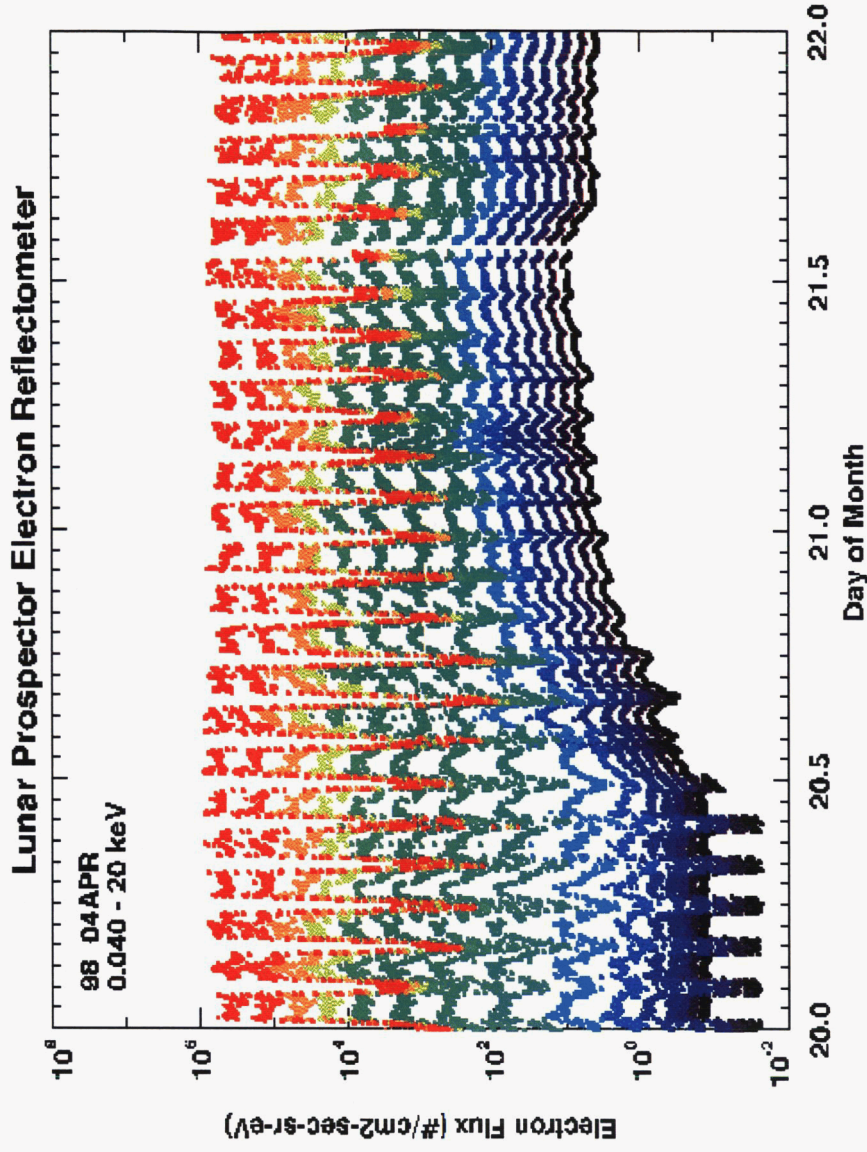


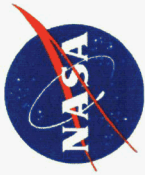


# Lunar Plasma Environments

---

- Lunar Prospector Electron Reflectometer
  - Spin average electron flux
  - ~40 eV to ~20 keV
- 4-5 April 1998
  - Moon in solar wind
  - Plasma wake
  - Solar particle event and wake





# Charging in Lunar Wake

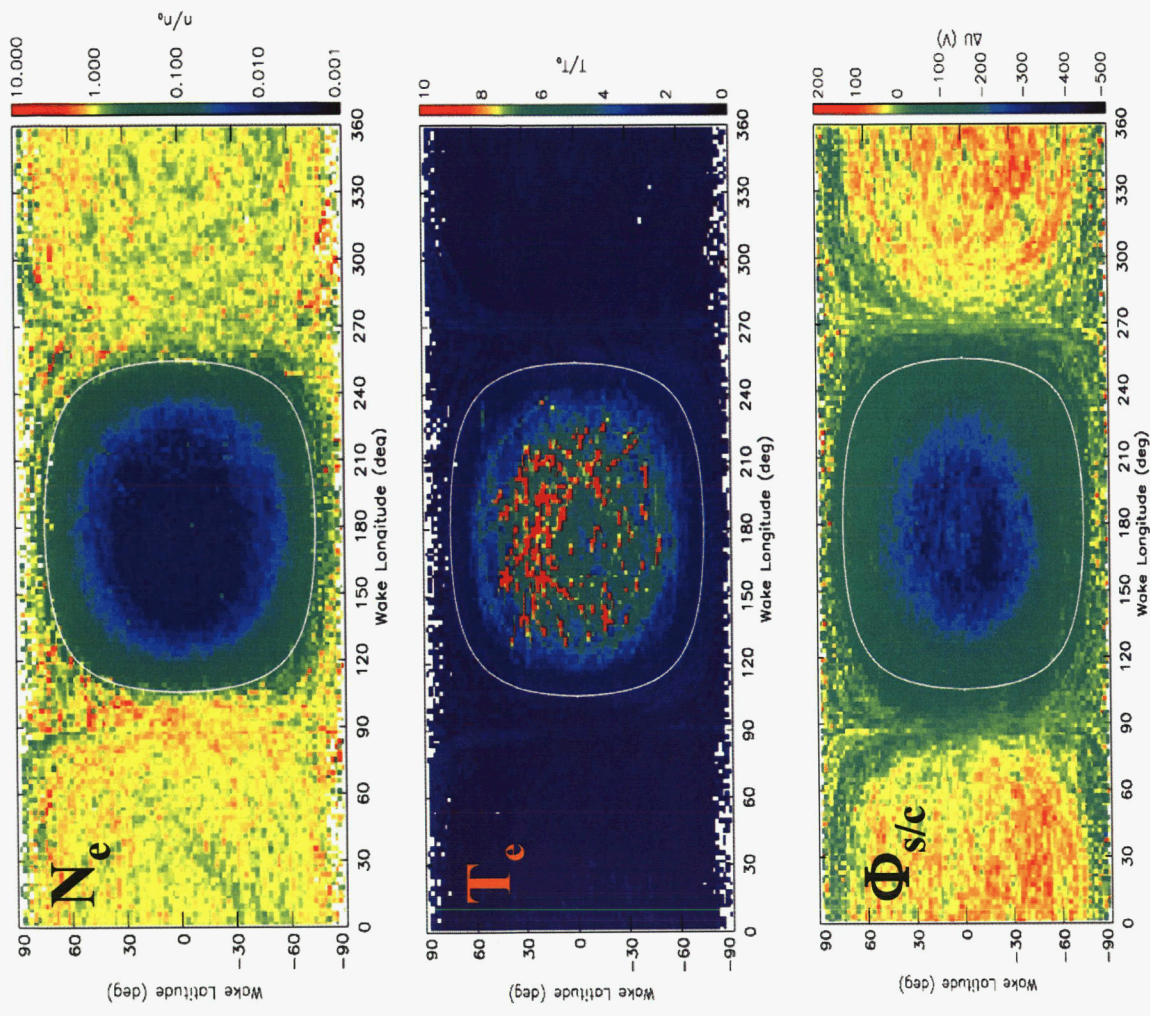
Lunar Prospector  
20-115 km

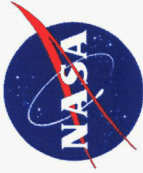
Wake properties relative  
to ambient solar wind

[Halekas et al. 2005]

Spacecraft potentials

day +10 V to +50V  
night -100 V to -300 V





# Summary

---

- **Libration orbit radiation and plasma environments dominated by solar wind, solar energetic particles, and galactic cosmic rays**
  - SPE, GCR considered relatively benign compared to trapped radiation belts
  - Plasma environments are interesting due to perturbations by terrestrial magnetic field, lunar wake
- Libration points are good locations for monitoring:
  - Solar input to Earth/Moon system
  - Magnetotail dynamics at lunar orbit distances
  - Foreshock phenomenon
- L2-CPE model developed by NASA/MSFC provides plasma environments to ~1 MeV for Sun-Earth/Moon L2 point
  - Sun-Earth/Moon L1, L3, L4, L5 available by disabling magnetotail environments
  - Lunar modification in work to include all lunar libration points